



Susceptibility of Two Southern Ocean Phytoplankton Key Species to Iron Limitation and High Light

Scarlett Trimborn^{1,2*}, Silke Thoms¹, Kai Bischof² and Sara Beszteri¹

¹ Biogeosciences Section, EcoTrace, Alfred Wegener Institute, Helmholtz Centre for Polar and Marine Research, Bremerhaven, Germany, ² Marine Botany Department, Faculty 2 Biology/Chemistry, University of Bremen, Bremen, Germany

OPEN ACCESS

Edited by:

Susana Agusti,
King Abdullah University of Science
and Technology, Saudi Arabia

Reviewed by:

Linn Hoffmann,
University of Otago, New Zealand
Alexandra Coello Camba,
King Abdullah University of Science
and Technology, Saudi Arabia

*Correspondence:

Scarlett Trimborn
scarlett.trimborn@awi.de

Specialty section:

This article was submitted to
Global Change and the Future Ocean,
a section of the journal
Frontiers in Marine Science

Received: 20 December 2018

Accepted: 15 March 2019

Published: 17 April 2019

Citation:

Trimborn S, Thoms S, Bischof K
and Beszteri S (2019) Susceptibility
of Two Southern Ocean
Phytoplankton Key Species to Iron
Limitation and High Light.
Front. Mar. Sci. 6:167.
doi: 10.3389/fmars.2019.00167

Although iron (Fe) availability primarily sets the rate of phytoplankton growth and primary and export production in the Southern Ocean, other environmental factors, most significantly light, also affect productivity. As light availability strongly influences phytoplankton species distribution in low Fe-waters, we investigated the combined effects of increasing light (20, 200, and 500 $\mu\text{mol photons m}^{-2} \text{s}^{-1}$) in conjunction with different Fe (0.4 and 2 nM) availability on the physiology of two ecologically relevant phytoplankton species in the Southern Ocean, *Chaetoceros debilis* (Bacillariophyceae) and *Phaeocystis antarctica* (Haptophyceae). Fe-deficient cells of *P. antarctica* displayed similar high growth rates at all irradiances. In comparison, Fe-deplete *C. debilis* cells grew much slower under low and medium irradiance and were unable to grow at the highest irradiance. Interestingly, Fe-deficient *C. debilis* cells were better protected against short-term excessive irradiances than *P. antarctica*. This tolerance was apparently counteracted by strongly lowered growth and particulate organic carbon production rates of the diatom relative to the prymnesiophyte. Overall, our results show that *P. antarctica* was the more tolerant species to changes in the availability of Fe and light, providing it a competitive advantage under a high light regime in Fe-deficient waters as projected for the future.

Keywords: climate change, growth, multiple stressors, photophysiology, photosynthesis, trace metals, *Chaetoceros*, *Phaeocystis*

INTRODUCTION

Even though the Southern Ocean (SO) represents the largest high nutrient low chlorophyll (HNLC) region of the world oceans, it is responsible for a large share of uptake and storage of anthropogenic CO_2 (Sabine et al., 2004; Landschützer et al., 2015). The drawdown of CO_2 via photosynthesis by SO phytoplankton accounts for $\sim 10\%$ of this uptake (Dunne et al., 2007). Even though there is ample supply of macronutrients, growth and primary production of SO phytoplankton is limited by the input of the trace element iron (Fe) (Martin et al., 1990), which is required for photosynthesis. The SO is currently undergoing climatic changes, which will influence SO phytoplankton ecology and biogeochemistry in a yet poorly understood manner. The rise in sea surface temperature and the subsequent sea ice melt is predicted to shallow the mixed layer depth (Meijers, 2014), causing on the one hand reduced trace metal input from deeper layers (Bopp et al., 2001) and on the other hand a higher irradiance regime that phytoplankton will encounter (Bopp et al., 2013).

In contrast, other climate model simulations predict a strengthening of the westerly winds (Meijers, 2014), which will deepen the mixed layer depth and reduce light availability for phytoplankton, but implying potentially also higher trace metal input from deeper layers (Hauck et al., 2015). The consequences of these climatic changes for SO phytoplankton productivity, however, remain poorly understood.

Changes in the availability of both light and Fe have a strong influence on phytoplankton physiology. For several temperate phytoplankton species, it has been shown that Fe limitation reduced the light use capacity under low light conditions due to the high Fe demand for the Fe-rich components of the photosynthetic apparatus such as photosystem I (PSI), cytochrome b6/f (Cytb6/f) and photosystem II (PSII) (PSI > Cytb6/f > PSII; Raven, 1990; Sunda and Huntsman, 1997, 2011). Recently, it was, however, demonstrated that this concept does not apply for SO phytoplankton species as low light intensities did not affect their cellular Fe requirements under Fe-limitation (Strzpek et al., 2012). In contrast to temperate phytoplankton species, which were found to increase the number of Fe-requiring photosynthetic units (e.g., PSI), SO species have evolved a different photoacclimation strategy as they increase their light harvesting size (Robinson et al., 1997; Kropuenske et al., 2010; Strzpek et al., 2012), requiring thereby no additional Fe supply. This strategy, however, has the disadvantage that it reduces the efficiency of excitation energy transfer from light-harvesting pigments to photosynthetic reaction centers (Raven, 1990) and could therefore be particularly stressful for SO phytoplankton under low Fe and high light conditions. While the physiological response of SO phytoplankton species to Fe limitation under low irradiance was assessed in several SO phytoplankton isolates in the laboratory (Timmermans et al., 2001; Hoffmann et al., 2008; Strzpek et al., 2012; Luxem et al., 2017), the implications of a low Fe and high light environment for SO key phytoplankton species has not been tested so far. To date, mainly shipboard incubation experiments were conducted, revealing that SO phytoplankton communities were characterized by a higher susceptibility to photoinhibition and lowered photosynthetic performance under these conditions (Moore et al., 2007; Alderkamp et al., 2010; Petrou et al., 2011; Van de Poll et al., 2011). Hence, SO phytoplankton thriving in low Fe high light environments, as projected for the future, need to balance between maintenance of high photosynthetic efficiency and prevention of photodamage due to constrains in light use efficiency.

The exposure of phytoplankton cells to high irradiances requires the dissipation of excess energy to prevent damage and the metabolically costly repair of PSII. Phytoplankton dissipate this energy through several pathways such as non-photochemical quenching (NPQ; Falkowski and Raven, 2007). NPQ includes the dissipation of energy triggered by the acidification of the thylakoid lumen, which induces the enzymatic conversion of the xanthophyll diadinoxanthin to diatoxanthin. Xanthophyll cycling is a common strategy of Antarctic diatoms and the prymnesiophyte *Phaeocystis antarctica* against excessive irradiance (Mills et al., 2010; Petrou et al., 2011; Van de Poll et al., 2011; Heiden et al., 2016; Trimborn et al., 2017; Heiden et al., 2018). As Fe is not required in the latter pathway, it is especially advantageous for phytoplankton in Fe-limited

waters. Cyclic electron transport around PSI represents another important pathway to alleviate excitation pressure, this pathway is, however, Fe intensive, requiring the Fe-containing PSI and cytochrome b6/f, and increases the likelihood of reactive oxygen production (Behrenfeld and Milligan, 2012). A much lower Fe requirement than the PSI cyclic pathway involves plastid terminal oxidases (PTOX), which transfer electrons to oxygen, generating thereby water and bypassing the Fe-rich PSI and cytochrome b6/f (Mackey et al., 2008). In particular for Fe-limited phytoplankton, this dissipation pathway was suggested to be beneficial (Mackey et al., 2008; Behrenfeld and Milligan, 2012), its role in SO species remains, however, yet unresolved.

To gain a detailed mechanistic understanding of how changes in Fe and light availability potentially shape SO phytoplankton distribution in the future, we assessed the physiological responses of the diatom *Chaetoceros debilis* and the prymnesiophyte *P. antarctica*, being relevant in both ecological as well as biogeochemical terms in the SO, and exposed them to different climatic scenarios. To this end, both species were grown under two Fe concentrations (0.4 and 2 nmol L⁻¹) in combination with three constant irradiance levels (20, 200, and 500 μmol photons m⁻² s⁻¹) and their combined effects on growth, production of particulate organic carbon and biogenic silica and photophysiology were assessed.

MATERIALS AND METHODS

Experimental Set-Up

Prior to the initiation of the experiment, the diatom *C. debilis* (Polarstern expedition 'EIFEX' ANT-XXI/3, In-Patch, 2004, 49° 36S, 02° 05E, isolated by Philipp Assmy) and the flagellate *P. antarctica* (solitary cells isolated by P. Pendoley in March 1992 at 68° 39S, 72° 21E) were kept for more than a year in stock cultures with Fe-deplete and -replete natural Antarctic seawater medium. For the preacclimation phase (over 2 weeks) and the main experiment, dilute batch cultures of *C. debilis* and *P. antarctica* were grown in natural low Fe (0.4 nmol L⁻¹) Antarctic seawater (sampled during Polarstern expedition ANT29-2 on September, 20, 2013, 60° 31.55' S 26° 29.06' W), to which a trace metal mix containing no (e.g., control treatment) or 2 nmol L⁻¹ Fe (FeCl₃, ICP-MS standard, TraceCERT, Fluka; e.g., +Fe treatment) was added. The trace metal mixture contained zinc (0.16 nmol L⁻¹), copper (0.08 nmol L⁻¹), cobalt (0.09 nmol L⁻¹ Co), molybdenum (0.05 nmol L⁻¹), and manganese (1.9 nmol L⁻¹). These trace metal additions were adjusted to maintain the ratio of the original F/2 recipe and represent trace metal concentrations typical for Antarctic HNLC waters. As suggested by Gerringa et al. (2000), in an effort to minimize the alteration of the natural seawater trace metal chemistry and ligands, no ethylenediaminetetraacetic acid (EDTA) was added. Due to the naturally present ligands (1.62 ± 0.20 nmol L⁻¹), it is expected that the added Fe was buffered rather than forming inorganic colloids. Prior to experiments, this seawater was sterile filtered through acid-cleaned filter cartridges (0.2 μm, Sartobran, Sartorius) and spiked with chelexed (Chelex[®] 100, Sigma-Aldrich, Merck) macronutrients (100 μmol L⁻¹ Si, 100 μmol L⁻¹ NO₃⁻, and 6.25 μmol L⁻¹ PO₄³⁻) and

vitamins (30 nmol L⁻¹ B₁, 23 nmol L⁻¹ B₇, and 0.228 nmol L⁻¹ B₁₂) according to F/2_R medium (Guillard and Ryther, 1962). To avoid any Fe contamination, all sampling and handling of the incubations was conducted under a laminar flow hood (Class 100, Opta, Bensheim, Germany) using trace metal clean techniques. Tubing, reservoir carboys, incubation bottles and other equipment were acid-cleaned prior use: After a 2-day Citranox detergent bath and subsequent rinsing steps with Milli-Q (MQ, Millipore), equipment was kept in acid (5 N HCl for polyethylene and 1 N HCl for polycarbonate materials) for 7 days, followed by 7 rinses with MQ. Equipment was kept triple-bagged during storage and experiments. In addition to the different Fe conditions, the two species were grown at an incident light intensity of 20, 200, and 500 μmol photons m⁻² s⁻¹ (LL, ML, and HL treatment, respectively) under a light:dark cycle of 16:8 h using light-emitting diodes (LED) lamps (SolarStinger LED SunStrip Marine Daylight, Econlux). Light intensities were adjusted using a LI-1400 datalogger (Li-Cor, Lincoln, NE, United States) with a 4π-sensor (Walz, Effeltrich, Germany). Apart from *C. debilis*, which was not able to grow under Fe-limitation in combination with HL conditions, triplicates of each experimental treatment were grown at 2°C. Both species were acclimated to each experimental condition for at least 2 weeks before start of the main experiments. The main experiments lasted between 18 and 22 days for control treatments and between 8 and 12 days for +Fe treatments of *C. debilis*. For *P. antarctica*, the main experiment took between 11 and 14 days for control treatments and between 9 and 10 days for the +Fe treatments.

Photophysiological Characteristics

By means of a Fast Repetition Rate fluorometer (FRRf, FastOcean PTX; Chelsea Technologies Group Ltd., West Molesey, United Kingdom) in combination with a FastAct Laboratory system (Chelsea Technologies Group Ltd., West Molesey, United Kingdom), the efficiency of photochemistry in photosystem II (PSII) was assessed in all treatments. Over the course of the experiment, cells of the respective treatment were dark-adapted for 10 min, before minimum fluorescence (F_0) was recorded. Subsequently, a single turnover flashlet (1.2 × 10²² photons m⁻² s⁻¹, wavelength 450 nm) was applied to cumulatively saturate photosystem II (PSII), i.e., a single photochemical turnover (Kolber et al., 1998). The single turnover saturation phase comprised 100 flashlets on a 2 μs pitch and was followed by a relaxation phase comprising 40 flashlets on a 50 μs pitch. This sequence was repeated 24 times within each acquisition. The saturation phase of the single turnover acquisition was fitted according to Kolber et al. (1998). From this measurement, the minimum (F_0) and maximum (F_m) fluorescence was determined in each sample. In addition to this, a blank of each sample was 0.2 μm filtered to assess background fluorescence. The dark-adapted maximum PSII quantum yield (F_v/F_m) was calculated after blank correction according to the equation $(F_m - F_0)/F_m$. At the end of the main experiment, cells were exposed for 5 min to eight actinic light levels ranging from 41 to 1205 μmol photons m⁻² s⁻¹ during fluorescence light curves (FLC). From these measurements, the light-adapted minimum (F') and maximum (F_m') fluorescence

of the single turnover acquisition was estimated. The effective PSII quantum yield under ambient light (F_q'/F_m') was derived according to the equation $(F_m' - F')/F_m'$ (Genty et al., 1989). From this curve, absolute electron transport rates (ETR, e⁻ PSII⁻¹ s⁻¹) were calculated following Suggett et al. (2004, 2009):

$$\text{ETR} = \sigma_{\text{PSII}} \times (F_q'/F_m'/F_v/F_m) \times E \quad (1)$$

where σ_{PSII} is the functional absorption cross section of PSII photochemistry and E denotes the applied instantaneous irradiance (photons m⁻² s⁻¹). Light-use characteristics were analyzed by fitting irradiance-dependent ETRs according to Ralph and Gademann (2005), including maximum ETR (ETR_{max}), minimum saturating irradiance (I_K) and maximum light utilization efficiency (α). Using the Stern-Volmer equation, non-photochemical quenching (NPQ) of chlorophyll *a* fluorescence was calculated as $F_m/F_m' - 1$. From the single turnover measurement of dark-adapted cells, σ_{PSII} , the energy transfer between PSII units (i.e., connectivity, P), the re-oxidation of the electron acceptor Q_a (τ) and the concentration of functional photosystem II reaction centers ([RII]) were assessed from iterative algorithms for induction (Kolber et al., 1998) and relaxation phase (Oxborough et al., 2012). [RII] represents an estimator for the content of PSII in the sample and was calculated according to the following equation:

$$[\text{RII}] = (F_0/\sigma_{\text{PSII}}) \times (K_R/E_{\text{LED}}) \quad (2)$$

where K_R is an instrument specific constant and E_{LED} is the photon flux from the FRRf measuring LEDs. After the completion of the FLC curve, an additional dark-adaptation period of 10 min was applied, followed by a single turnover flashlet to check for recovery of PSII. Using the F_v/F_m measured before and after the FLC-curve, the yield recovery was calculated and given as % of the initial F_v/F_m (before the FLC-curve). All measurements ($n = 3$) were conducted at the growth temperature of 2°C.

Growth and Cell Size Determination

Cell count samples of each treatment were taken on a daily basis at the same time of the day. While cell size, volume and numbers for the solitary *P. antarctica* were determined immediately after sampling using a Coulter Multisizer III (Beckman Coulter, Fullerton, CA, United States), cell count samples of the chain-forming *C. debilis* were fixed with 10% acid lugol's solution and stored at 2°C in the dark until counting. Cell numbers of *C. debilis* were estimated according to the method by Utermöhl (1958) using 3 ml sedimentation chambers (Hydro-Bios, Kiel, Germany) on an inverted microscope (Zeiss Axiovert 200) counting at least 400 cells in transects.

Cell-specific growth rate (μ , unit d⁻¹) was calculated as

$$\mu = (\ln N_{\text{fin}} - \ln N_0)/\Delta t \quad (3)$$

where N_0 and N_{fin} denote the cell concentrations at the beginning and the end of the experiments, respectively, and Δt is the corresponding duration of incubation in days. Both species grew exponentially and at the time of harvest cell densities ranged

between 75,000 and 128,000 cells per mL for *P. antarctica* and 63,000 and 134,000 cells per mL for *C. debilis*. Cellular biovolume was measured from cell count samples taken at the end of the experiment using the Coulter Multisizer III for *P. antarctica* and inverted microscopy for *C. debilis* and was calculated according to Hillebrand et al. (1999).

Elemental Composition and Stoichiometry

On the final day of the experiment, samples for determination of particulate organic carbon (POC) and particulate organic nitrogen (PON) were taken filtering cells onto precombusted (15 h, 500 °C) glass fiber filters (GF/F, pore size ~0.6 µm, Whatman). Filters were stored at -20°C and dried for >12 h at 60°C prior to sample preparation. Analysis was performed using an Euro Vector CHNS-O elemental analyzer (Euro Elemental Analyzer 3000, HEKAtech GmbH, Wegberg, Germany). Contents of POC and PON were corrected for blank measurements and normalized to filtered volume and cell densities to yield cellular quotas. Samples for the determination of biogenic silica (BSi) were taken also on the final day of the experiment and filtered through a cellulose acetate filter (Sartorius, 0.4 µm) and stored at -20°C. The filters were then digested in 0.2 N NaOH, at 95°C for 60 min, neutralized with 1 M HCl according to Brzezinski and Nelson (1995) and analyzed colorimetrically for silicate using standard spectrophotometric techniques (Koroleff, 1983). BSi content was normalized to filtered volume and cell density. Production rates of POC, PON, and BSi were calculated by multiplication of the cellular quota with the specific growth rate of the respective treatment.

Pigments

Samples for the determination of pigment concentration were taken on the final day of the experiment and filtered onto GF/F filters and immediately frozen at -80°C until further analysis. Pigments samples were homogenized and extracted in 90% acetone for 24 h at 4°C in the dark. After centrifugation (5 min, 4°C, 13,000 rpm) and filtration through a 0.45 µm pore size nylon syringe filter (Nalgene®, Nalge Nunc International, Rochester, NY, United States), concentrations of chlorophyll *a* (Chl *a*) and *c*₂ (Chl *c*₂), fucoxanthin (Fuco), diatoxanthin (Dt), and diadinoxanthin (Dd) were determined by reversed phase High Performance Liquid Chromatography (HPLC). The analysis was performed on a LaChrom Elite® system equipped with a chilled autosampler L-2200 and a DAD detector L-2450 (VWR-Hitachi International GmbH, Darmstadt, Germany). A Spherisorb® ODS-2 column (25 cm × 4.6 mm, 5 µm particle size; Waters, Milford, MA, United States) with a LiChropher® 100-RP-18 guard cartridge was used for the separation of pigments, applying a gradient according to Wright et al. (1991). Peaks were detected at 440 nm and identified as well as quantified by co-chromatography with standards for Chl *a* and *c*₂, Fuco, Dt, and Dd (DHI Lab Products, Hørsholm, Denmark) using the software EZChrom Elite ver. 3.1.3. (Agilent Technologies, Santa Clara, CA, United States). Pigment contents were normalized to filtered volume and cell densities to yield cellular quotas.

Statistics

Combined effects of the two Fe (control and Fe-enriched) and light (LL, ML, and HL) treatments on all experimental parameters were statistically analyzed using two-way analyses of variance (ANOVA) with Bonferroni's multiple comparison *post hoc* tests. To test for significant differences between light treatments of Fe-enriched *C. debilis* cells one-way ANOVAs with additional Bonferroni's multiple comparison *post hoc* tests were applied. All statistical analyses were performed using the program GraphPad Prism (Version 5.00 for Windows, Graph Pad Software, San Diego, CA, United States) and the significance testing was done at the $p < 0.05$ level.

RESULTS

Maximum Quantum Yield and Functional Absorption Cross-Sections of PSII

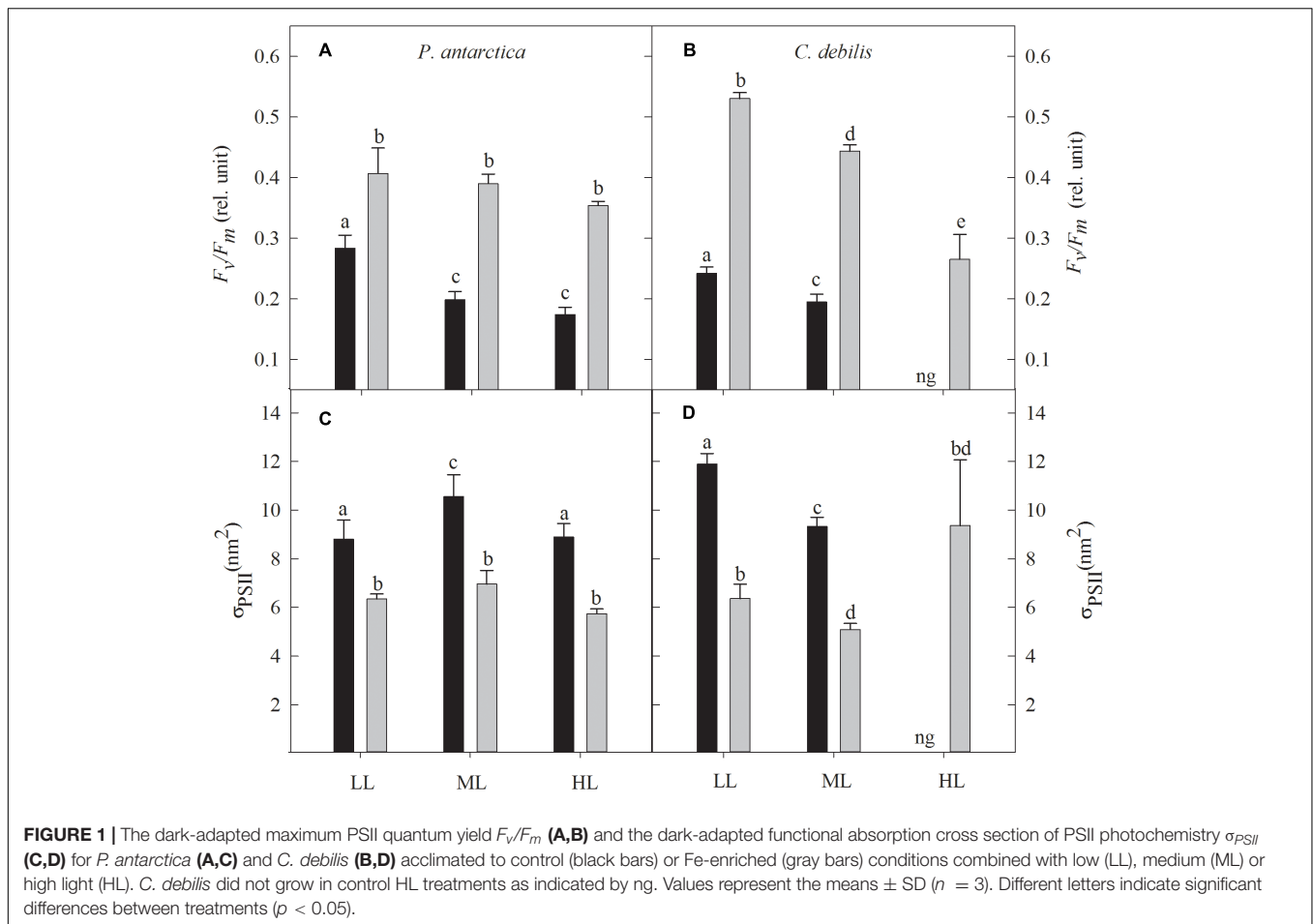
The dark-adapted maximum quantum yield of PSII (F_v/F_m) was strongly influenced by Fe addition, being significantly enhanced in all light treatments of both species (**Figures 1A,B**; 2-way ANOVA: $p < 0.0001$). In response to increasing light, also strong species-specific effects were observed. For *P. antarctica*, F_v/F_m did not change in response to increasing light except for the control treatments, which were significantly reduced by 29% between LL and ML (*post hoc*: $p < 0.01$). For *C. debilis*, with increasing irradiance F_v/F_m values significantly declined in control and +Fe treatments (2-way ANOVA: $p < 0.0001$).

In response to Fe-enrichment, functional absorption cross-sections of PSII (σ_{PSII}) were significantly reduced in both species (**Figures 1C,D**; 2-way ANOVA: $p < 0.0001$). With increasing light, σ_{PSII} was differently affected among the two species. For *P. antarctica*, σ_{PSII} remained unaltered in +Fe treatments while for control treatments σ_{PSII} increased by 20% from LL to ML (*post hoc*: $p < 0.05$), but declined by 16% from ML to HL (*post hoc*: $p < 0.05$). For *C. debilis*, σ_{PSII} significantly declined from LL to ML in all treatments (2-way ANOVA: $p < 0.0001$), but remained unaltered between ML and HL in the +Fe treatments.

Cell Volume, Growth, Elemental Composition and Stoichiometry

Cell volumes of *P. antarctica* and *C. debilis* were significantly increased after Fe-enrichment (*P. antarctica*: 2-way ANOVA: $p < 0.0001$, *C. debilis*: 2-way ANOVA: $p = 0.003$) except for the ML treatment of *C. debilis* (**Figures 2A,B**). Cell volume did not change in response to increasing light intensity in all treatments of *C. debilis*. For *P. antarctica*, cell volume significantly increased in all treatments between LL and ML (2-way ANOVA: $p < 0.0001$), but remained unaltered toward HL.

Growth rates of *P. antarctica* and *C. debilis* were differently affected by Fe and light (**Figures 2C,D**). In response to Fe-enrichment, growth rates of *P. antarctica* were significantly enhanced at LL and ML (2-way ANOVA: $p = 0.0005$), but remained unaltered at HL. In comparison, *C. debilis* showed a Fe-dependent increase in growth under ML (*post hoc*: $p < 0.01$), but not under LL. When grown under control conditions in



combination with HL, *C. debilis* was not able to grow. In response to increasing light intensity, growth rates did not change in *P. antarctica*. In comparison, growth rates of *C. debilis* increased with increasing light intensity under +Fe conditions (2-way ANOVA: $p = 0.0033$), but this trend was only significant between LL and ML (*post hoc*: $p < 0.05$) and not between ML and HL.

For both species, POC production rates were differently affected by the availability of Fe and light (Figures 2E,F). Enrichment with Fe significantly enhanced POC production rates in all light treatments of *P. antarctica* and *C. debilis* (2-way ANOVA: $p < 0.0001$). In response to increasing light, daily POC production remained generally unaltered in *C. debilis*. Only from ML to HL, +Fe treatments of *C. debilis* showed an increase in POC production by 42% (*post hoc*: $p < 0.05$). In comparison, POC production rates of *P. antarctica* did not change with increasing light intensity in the control treatments. For the +Fe treatments of *P. antarctica*, POC production was significantly enhanced by 15% between LL and ML (*post hoc*: $p < 0.05$), but significantly declined by 15% between ML and HL (*post hoc*: $p < 0.05$).

Among species, ratios of C:N varied depending on the availability of Fe and light (Table 1). Fe enrichment did generally not alter C:N ratios in *P. antarctica* and *C. debilis*. Only for the latter, Fe-enrichment reduced C:N ratios by 18% at LL (*post hoc*: $p < 0.0001$). With increasing light, C:N ratios were similar among

control treatments of both species. For the +Fe treatments, C:N ratios also did not change between ML and HL. From LL to ML, C:N ratios significantly declined by 6% in *P. antarctica* (*post hoc*: $p < 0.05$) while they significantly increased by 20% in *C. debilis* (*post hoc*: $p < 0.0001$).

For *C. debilis*, in response to Fe-enrichment BSi production rates remained unchanged at LL, but significantly increased at ML (*post hoc*: $p < 0.001$, Figure 2G). With increasing light intensity, BSi production rates were not affected in control treatments whereas they were significantly enhanced in +Fe treatments (1-way ANOVA: $p < 0.0003$). Ratios of BSi:C resulted in an Fe-dependent decline by 84 and 48% in LL and ML treatments, respectively (2-way ANOVA: $p < 0.0001$, Table 1). With increasing irradiance, BSi:C ratios did not change for control conditions while there was a significant light-dependent increase in +Fe treatments (1-way ANOVA: $p < 0.0004$).

Cellular Pigment Concentrations

Cellular concentrations of chlorophyll *a* (Chl *a*) were enhanced by Fe addition in *P. antarctica* (2-way ANOVA: $p < 0.0001$, Table 1) and *C. debilis* (2-way ANOVA: $p = 0.0009$, Table 1) even though for the latter this trend was not significant at ML. Between LL and ML Chl *a* quotas decreased in the +Fe treatments of both species (*P. antarctica*: 2-way ANOVA: $p < 0.0001$, *C. debilis*: 2-way ANOVA: $p = 0.0006$).

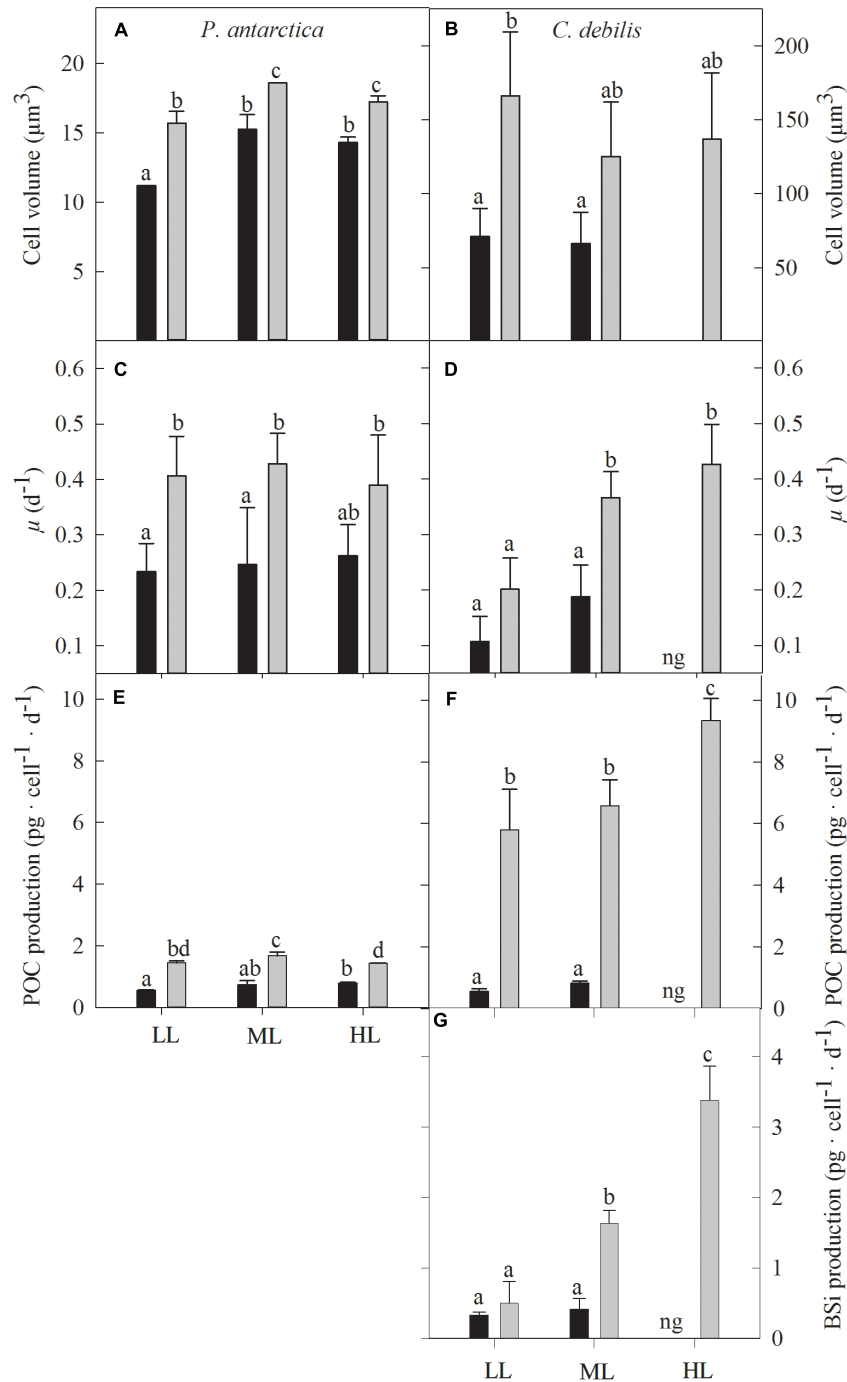


FIGURE 2 | Cell volume (A,B), growth rate (C,D), cellular production rate of particulate organic carbon (E,F) and biogenic silica (G) for *P. antarctica* (A,C,E) and *C. debilis* (B,D,F,G) acclimated to control (black bars) or Fe-enriched (gray bars) conditions combined with low (LL), medium (ML) or high light (HL). *C. debilis* did not grow in control HL treatments as indicated by ng. Values represent the means \pm SD ($n = 3$). Different letters indicate significant differences between treatments ($p < 0.05$).

Such light-dependent trend in Chl *a* quotas was also seen in control treatment of both species, even though not found to be statistically significant. Between ML and HL Chl *a* quotas remained constant in the +Fe treatments of both species.

Cellular chlorophyll *c*₂ (Chl *c*₂) concentrations were generally not altered in response to Fe enrichment (Table 1). Only at LL, Fe addition led to a significant increase of the Chl *c*₂ quotas in both species (for *P. antarctica*: *post hoc*: $p < 0.05$, for *C. debilis*: *post hoc*: $p < 0.001$). Increasing light did generally not affect Chl *c*₂ quotas

TABLE 1 | Molar ratios of C:N, BSi:C as well as cellular quotas of chlorophyll a (Chl a), chlorophyll c₂ (Chl c₂), fucoxanthin (Fuco), and diadinoxanthin (Dd) were determined for *P. antarctica* and *C. debilis* acclimated to control and Fe-enriched conditions combined with low (LL), medium (ML) or high light (HL).

| Treatment | C:N (mol mol ⁻¹) | BSi:C (mol mol ⁻¹) | Chl a (fg cell ⁻¹) | Chl c ₂ (fg cell ⁻¹) | Fuco (fg cell ⁻¹) | Dd (fg cell ⁻¹) |
|----------------------|------------------------------|--------------------------------|--------------------------------|---|-------------------------------|-----------------------------|
| <i>P. antarctica</i> | | | | | | |
| Control LL | 5.6 ± 0.1 ^a | | 28.7 ± 1.2 ^a | 5.7 ± 3.9 ^a | 30.0 ± 0.9 ^a | 5.4 ± 0.5 ^a |
| Fe LL | 5.7 ± 0.1 ^a | | 77.2 ± 9.1 ^b | 10.3 ± 0.7 ^b | 29.7 ± 7.4 ^a | 4.7 ± 0.5 ^a |
| Control ML | 5.5 ± 0.1 ^{ab} | | 20.3 ± 2.7 ^{ab} | 3.6 ± 0.6 ^{ac} | 15.5 ± 1.7 ^b | 10.7 ± 0.9 ^{bc} |
| Fe ML | 5.4 ± 0.0 ^b | | 37.3 ± 1.6 ^c | 2.4 ± 0.1 ^c | 16.7 ± 0.8 ^b | 11.4 ± 1.8 ^{bc} |
| Control HL | 5.4 ± 0.2 ^{ab} | | 12.5 ± 1.1 ^b | 1.3 ± 0.3 ^c | 7.3 ± 0.4 ^b | 10.6 ± 2.3 ^b |
| Fe HL | 5.3 ± 0.1 ^b | | 28.0 ± 3.6 ^c | 1.7 ± 0.6 ^c | 9.6 ± 1.9 ^b | 14.9 ± 1.6 ^c |
| <i>C. debilis</i> | | | | | | |
| Control LL | 6.8 ± 0.2 ^a | 0.25 ± 0.02 ^a | 33.5 ± 3.3 ^a | 4.3 ± 0.6 ^a | 26.5 ± 2.2 ^a | 6.3 ± 0.7 ^a |
| Fe LL | 5.6 ± 0.0 ^b | 0.04 ± 0.01 ^b | 420.9 ± 135.5 ^b | 85.8 ± 23.9 ^b | 214.3 ± 64.5 ^b | 49.8 ± 12.9 ^b |
| Control ML | 6.6 ± 0.1 ^a | 0.21 ± 0.07 ^a | 3.6 ± 0.6 ^a | 1.7 ± 0.1 ^a | 9.7 ± 1.3 ^a | 8.1 ± 1.6 ^a |
| Fe ML | 6.7 ± 0.1 ^a | 0.11 ± 0.02 ^b | 18.8 ± 2.8 ^a | 10.2 ± 3.9 ^{ac} | 29.9 ± 8.8 ^c | 37.4 ± 13.9 ^b |
| Control HL | ng | ng | ng | ng | ng | ng |
| Fe HL | 6.7 ± 0.1 ^a | 0.15 ± 0.02 ^c | 9.9 ± 2.2 ^a | 8.4 ± 1.5 ^c | 21.3 ± 4.3 ^c | 50.8 ± 12.3 ^b |

C. debilis did not grow in control HL treatments as indicated by ng. Values represent the means ± SD (*n* = 3). Different letters indicate significant differences between treatments (*p* < 0.05).

of both species, except for the +Fe treatments, which showed a decline by 77 and 86% between LL and ML in *P. antarctica* (*post hoc*: *p* < 0.05) and *C. debilis* (*post hoc*: *p* < 0.05), respectively.

In response to different Fe and light availability, species-specific effects in cellular fuco concentrations were found (Table 1). In *P. antarctica* the addition of Fe did not change fucoxanthin quotas at all tested light levels. In comparison, Fuco quotas of *C. debilis* were enhanced in +Fe relative to control conditions, but only statistically significant at LL (*post hoc*: *p* < 0.01). From LL to ML fuco quotas generally declined in both species (*P. antarctica*: 2-way ANOVA: *p* = 0.4934, *C. debilis*: 2-way ANOVA: *p* = 0.0083) except for the control treatment of *C. debilis*. From ML to HL, fucoxanthin per cell did not change in both species.

Changes in light and Fe availability differently affected cellular concentrations of diadinoxanthin in both species (Table 1). While Fe availability did not alter cellular diadinoxanthin contents in *P. antarctica*, for *C. debilis* Fe-enrichment resulted in a strong increase of diadinoxanthin per cell in all light treatments (2-way ANOVA: *p* = 0.0004). From LL to ML, diadinoxanthin quotas of *P. antarctica* significantly increased in all treatments (2-way ANOVA: *p* < 0.0001), but did not change between ML and HL. For *C. debilis*, increasing light intensity had no influence on diadinoxanthin quotas.

Chlorophyll a Fluorescence

The energy transfer between PSII units (i.e., connectivity, *P*) showed species-specific effects in response to different Fe availability (Table 2). Whereas Fe-enrichment led to a significant increase of *P* in all light treatments of *C. debilis* (2-way ANOVA: *p* < 0.0001), there was no Fe-dependent change for *P. antarctica*. With increasing irradiance, *P* remained generally unaltered except for the +Fe treatments of *C. debilis*, which exhibited a decline by 31% from ML to HL (*post hoc*: *p* < 0.01). As a result of Fe-enrichment, cellular concentrations of functional photosystem II reaction centers ([RCII]) (Table 2) generally

increased in both species (2-way ANOVA: *p* < 0.0001). Only at ML and HL [RCII] did not change with Fe addition in *P. antarctica*. Increasing light generally reduced [RCII] in the two species (*P. antarctica*: 2-way ANOVA: *p* < 0.0001, *C. debilis*: 2-way ANOVA: *p* = 0.0005). Such light-dependent trends were also observed between ML and HL for *P. antarctica* and *C. debilis*, but being not statistically significant.

Fluorescence light curves showed clear species-specific differences in both shape and amplitude in response to changes in Fe and light availability (Figure 3). Maximum absolute electron transport rates (ETR_{max}) of both species did not differ between control and +Fe treatments apart from the ML treatment of *P. antarctica*, which exhibited an Fe-dependent decline by 32% (*post hoc*: *p* < 0.05) (Table 2). Acclimation of both species to increasing irradiance affected ETR_{max} differently. For *P. antarctica*, ETR_{max} generally increased with increasing light intensity (2-way ANOVA: *p* < 0.0001). Such trend was also seen between ML and HL in control treatments of *P. antarctica*, but was not statistically significant. For *C. debilis*, irrespective of the Fe availability ETR_{max} values were similar between LL and ML, but increased threefold from ML to HL in the +Fe treatments (*post hoc*: *p* < 0.05). Apart from the HL treatments of *P. antarctica*, which showed an Fe-dependent increase of 53% (*post hoc*: *p* < 0.01), the minimum saturating irradiance (*I*_K) was not influenced by Fe enrichment in both species (Table 2). Also, *I*_K values were similar among light treatments of both species except for the +Fe treatment of *P. antarctica*, where *I*_K increased from ML to HL (*post hoc*: *p* < 0.001).

Fe availability strongly influenced the maximum light utilization efficiency (*α*, Table 2), resulting in lowered *α* values after Fe enrichment in *C. debilis* (2-way ANOVA: *p* < 0.0004) and *P. antarctica* (2-way ANOVA: *p* = 0.0001). Only for the latter, when grown at LL, *α* values did not change between control and +Fe treatments. Light availability affected *α* in the two tested species differently. For *P. antarctica*, *α* was enhanced by 59% from LL to ML in control treatments (*post hoc*: *p* < 0.01) while

TABLE 2 | Energy transfers between PSII units (i.e., connectivity, P), cellular concentrations of functional photosystem II reaction centers ([RCII]), maximum electron transport rates (ETR_{max}), minimum saturating irradiances (I_k), maximum light utilization efficiencies (α) and F_v/F_m recovery were determined for *P. antarctica* and *C. debilis* acclimated to control or Fe-enriched conditions combined with low (LL), medium (ML) or high light (HL).

| Treatment | P (rel. unit) | [RCII] (zmol cell ⁻¹) | ETR_{max} (e ⁻ PSII ⁻¹ s ⁻¹) | I_k (μ mol photons m ⁻² s ⁻¹) | α (rel. unit) | F_v/F_m recovery (%) |
|----------------------|--------------------------|-----------------------------------|--|---|---------------------------|------------------------|
| <i>P. antarctica</i> | | | | | | |
| Control LL | nd | 61 ± 4 ^a | 192 ± 31 ^a | 42 ± 6 ^a | 4.82 ± 0.50 ^{ab} | 43 ± 10 ^a |
| Fe LL | 0.25 ± 0.05 ^a | 132 ± 3 ^b | 146 ± 10 ^a | 40 ± 7 ^a | 3.67 ± 0.43 ^a | 63 ± 15 ^{ab} |
| Control ML | 0.16 ± 0.06 ^a | 34 ± 12 ^c | 528 ± 91 ^b | 77 ± 18 ^{ab} | 7.64 ± 1.12 ^c | 36 ± 8 ^a |
| Fe ML | 0.25 ± 0.05 ^a | 22 ± 6 ^c | 360 ± 137 ^c | 74 ± 26 ^a | 4.89 ± 0.53 ^a | 56 ± 3 ^b |
| Control HL | 0.14 ± 0.06 ^a | 18 ± 8 ^c | 619 ± 29 ^b | 101 ± 16 ^b | 6.22 ± 0.84 ^{bc} | 42 ± 4 ^a |
| Fe HL | 0.25 ± 0.04 ^a | 17 ± 5 ^c | 563 ± 32 ^b | 155 ± 12 ^c | 3.64 ± 0.10 ^a | 57 ± 6 ^{ab} |
| <i>C. debilis</i> | | | | | | |
| Control LL | 0.21 ± 0.02 ^a | 60 ± 7 ^a | 915 ± 154 ^a | 190 ± 56 ^a | 4.93 ± 0.60 ^a | 74 ± 2 ^a |
| Fe LL | 0.45 ± 0.01 ^b | 223 ± 12 ^b | 862 ± 300 ^a | 250 ± 66 ^a | 3.41 ± 0.27 ^b | 50 ± 12 ^b |
| Control ML | 0.18 ± 0.04 ^a | 49 ± 8 ^a | 1083 ± 121 ^a | 308 ± 14 ^a | 3.51 ± 0.31 ^b | 85 ± 6 ^a |
| Fe ML | 0.39 ± 0.03 ^b | 131 ± 27 ^c | 671 ± 151 ^a | 262 ± 68 ^a | 2.57 ± 0.10 ^c | 61 ± 8 ^b |
| Control HL | ng | ng | ng | ng | ng | ng |
| Fe HL | 0.27 ± 0.04 ^c | 137 ± 9 ^c | 2232 ± 489 ^b | 351 ± 68 ^a | 6.37 ± 0.94 ^d | 113 ± 20 ^c |

C. debilis did not grow in control HL treatments as indicated by ng. For control LL treatments of *P. antarctica*, no measurements of P could be derived as indicated by nd. Photosynthetic parameters from photosynthesis irradiance curves were derived from at least three independent measurements. Different letters indicate significant differences between treatments ($p < 0.05$).

for all other treatments light had no influence. In comparison, in *C. debilis* α values decreased from LL to ML in control (*post hoc*: $p < 0.01$) and +Fe (*post hoc*: $p < 0.05$) treatments, but increased 2.5-fold from ML to HL in the +Fe treatments (*post hoc*: $p < 0.0001$).

Using the F_v/F_m measured before and after the FLC-curve, the F_v/F_m recovery was calculated and given as % of the initial F_v/F_m (before the FLC-curve). The recovery of F_v/F_m strongly differed among species (Table 2). In *P. antarctica*, the yield recovery was not influenced by the availability of Fe apart from the ML treatments, being significantly enhanced by 57% following Fe addition (*post hoc*: $p < 0.05$). For *C. debilis*, the yield recovery was significantly reduced in +Fe compared to control treatments under LL (*post hoc*: $p < 0.05$) and ML (*post hoc*: $p < 0.01$). In response to increasing light during acclimation, the capacity for yield recovery remained the same in both species. Only for Fe-enriched cells of *C. debilis*, the yield recovery significantly increased by 85% between ML and HL (*post hoc*: $p < 0.05$).

Large differences in re-oxidation times of the primary electron acceptor Q_a (τ_{Q_a}) among species existed with respect to changes in Fe and light availability (Figure 4). While for *P. antarctica* the addition of Fe did not affect τ_{Q_a} , for *C. debilis* under these conditions much longer re-oxidation times were observed (2-way ANOVA: $p = 0.0001$). In response to increasing irradiance during acclimation, τ was differently affected in *P. antarctica* than in *C. debilis*. For *P. antarctica*, re-oxidation times were much slower in control (*post hoc*: $p < 0.01$) and +Fe (*post hoc*: $p < 0.01$) treatments between LL and ML, but remained unaltered from ML to HL. In comparison, *C. debilis* exhibited much longer re-oxidation times in control (*post hoc*: $p < 0.05$) and +Fe (*post hoc*: $p < 0.01$) treatments between LL and ML while they were shortened between ML and HL in the +Fe treatments (*post hoc*: $p < 0.05$).

In both species, non-photochemical quenching (NPQ) generally went up with increasing actinic irradiance during the fluorescence irradiance curve (FLC, Figure 5). In response to

Fe-enrichment, diverging patterns in NPQ between *C. debilis* and *P. antarctica* were observed. Except for LL-acclimated cells, NPQ values were generally higher in +Fe than in control treatments of *P. antarctica* (Figures 5A,B). For *C. debilis*, the opposite trend was found (Figures 5C,D). With increasing irradiance, different species specific responses were observed. Among the different light treatments, in *C. debilis* NPQ values remained similar high independent of the Fe availability. *P. antarctica* on the other hand showed diverging light-dependent trends between control and +Fe treatments. While in this species NPQ activity was lowest for LL and highest for ML treatments in the +Fe treatments, the opposite trend was observed for the control treatments.

DISCUSSION

While previous studies mainly concentrated on the combined effect of Fe limitation and low irradiance (Timmermans et al., 2001; Hoffmann et al., 2008; Strzepak et al., 2012; Schuback et al., 2015; Luxem et al., 2017), this is the first laboratory study that assessed the physiological responses of the two ecologically important species *C. debilis* and *P. antarctica* in response to the combined effects of Fe limitation and high irradiance. Here, we discuss the influence and interaction of these two environmental factors on growth, POC production and photophysiology and their implications for the species occurrence in the present and future SO.

Species–Species Abilities to Cope With High Light Under Fe-Enriched Conditions

The acclimation to increasing irradiances imposed strong species-specific changes on their physiology. In contrast to *P. antarctica*, for which F_v/F_m remained unaltered in response to increasing irradiance in the +Fe treatments (Figure 1A), strong light effects on F_v/F_m were apparent in *C. debilis* despite Fe enrichment (Figure 1B). In the latter, with increasing irradiance

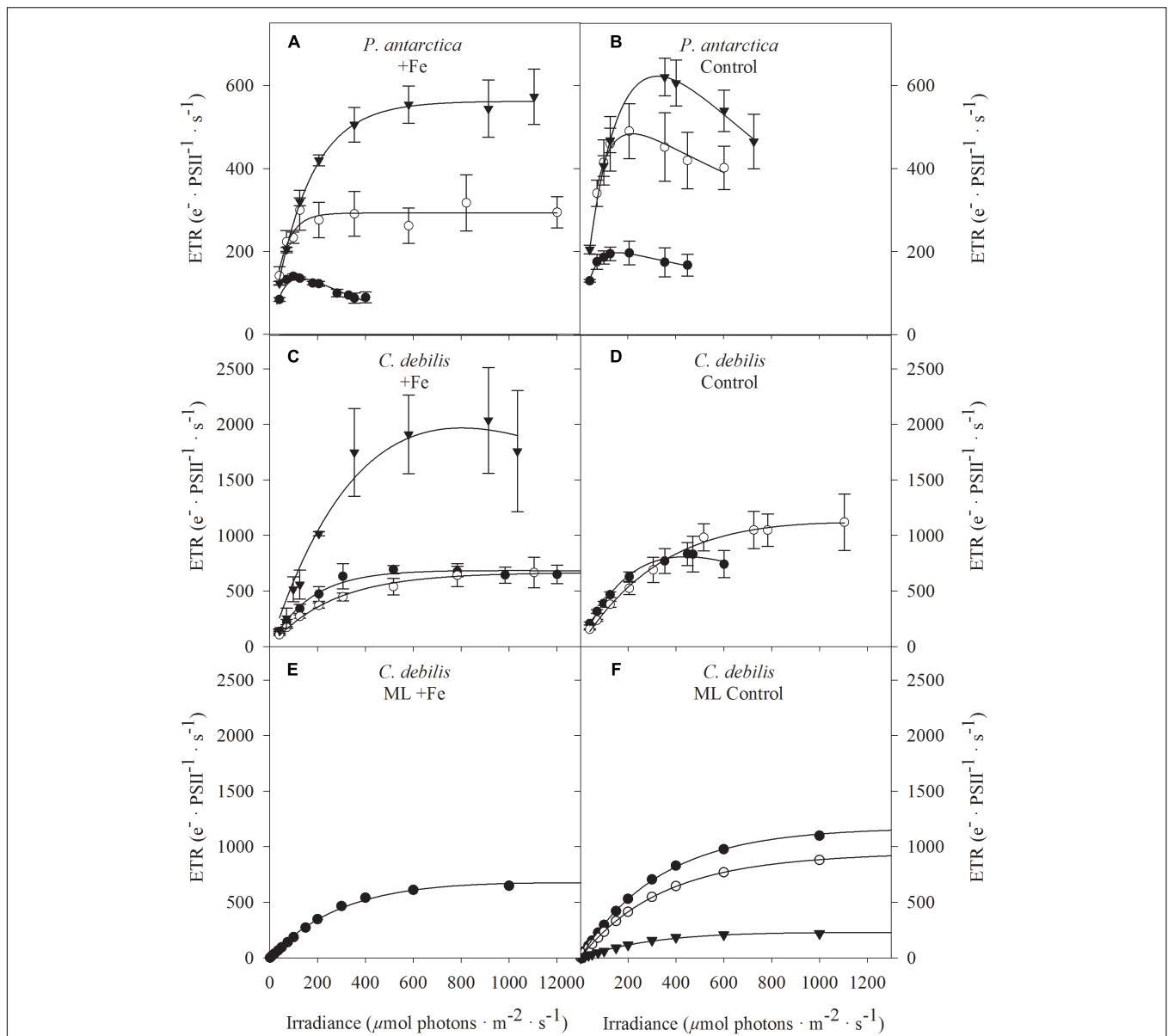
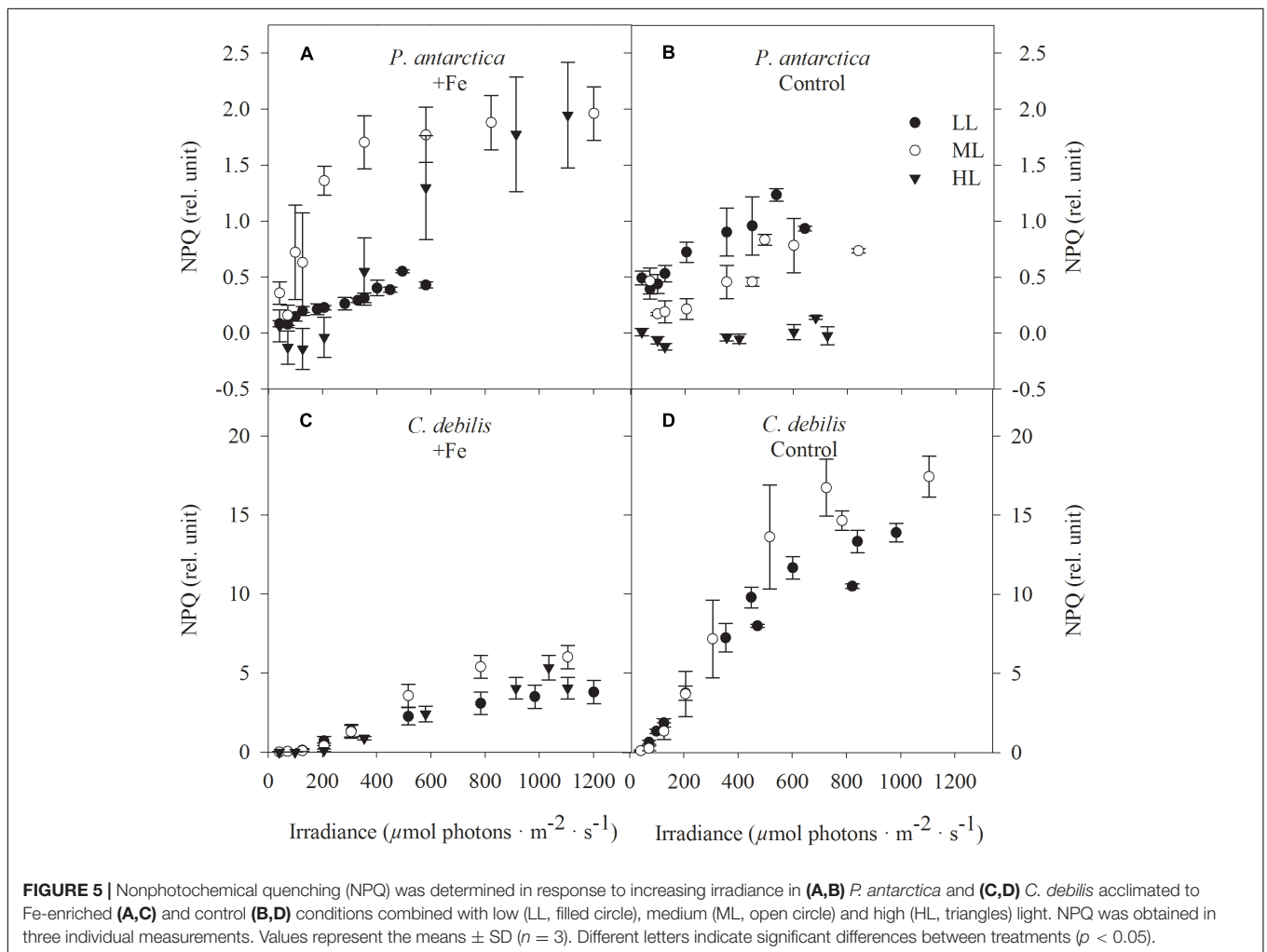
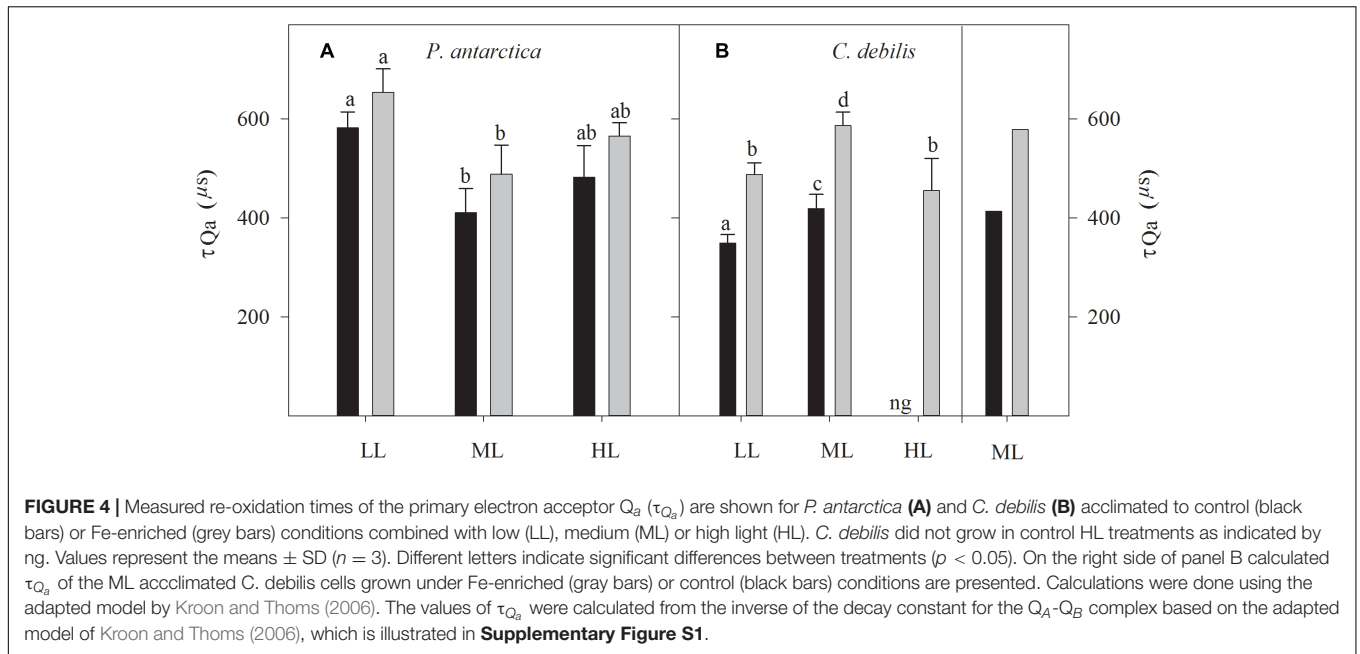


FIGURE 3 | Absolute electron transport rates (ETR) were measured in response to increasing irradiance in **(A,B)** *P. antarctica* and **(C,D)** *C. debilis* acclimated to Fe-enriched **(A,C)** and control **(B,D)** conditions combined with low (LL, filled circles), medium (ML, open circles) and high (HL, triangles) light. ETRs were obtained in three individual measurements. Values represent the means \pm SD ($n = 3$). Different letters indicate significant differences between treatments ($p < 0.05$). Using the model of Kroon and Thoms (2006), which was adapted to diatoms, total absolute ETRs (filled circles) were calculated by the example of ML acclimated *C. debilis* cells, which were grown under Fe-enriched **(E)** or control **(F)** conditions. The simulations are based on antenna scenarios and the amount of oxidized plastoquinone (PQ) as described in detail in **Supplementary Table S2**. In panel F, also the contribution of linear (triangles) versus putative plastid plastoquinol terminal oxidase (PTOX) activity (open circles) relative to the total ETRs is shown.

F_v/F_m strongly declined in the +Fe treatments, with the lowest value observed at HL. Similar light-dependent reductions in F_v/F_m even though Fe was added to the cultures were previously reported for various SO phytoplankton species (Arrigo et al., 2010; Mills et al., 2010; Strzpek et al., 2012; Heiden et al., 2016; Trimborn et al., 2017). In line with the unchanged photochemical efficiency, HL conditions did not alter growth of *P. antarctica* (Figure 2C), as previously observed for this

species (Trimborn et al., 2017) and another *P. antarctica* strain (Moisan and Mitchell, 1999) under Fe-replete conditions. We also observed changes in its daily POC production in this study, with a stimulative light effect between LL and ML (Figure 2E). The more efficient energy transfer from photochemistry to biomass production was further evident under these conditions by the faster re-oxidation times of the primary electron acceptor Q_a (τ_{Qa}) (Figure 4A) and the higher ETR_{max} (Table 2). As



a result from higher light availability at ML, cellular quotas related to light harvesting pigments (fucoxanthin, chlorophyll *a* and *c*₂, **Table 1**) were strongly reduced while those related to light protection (diadinoxanthin, **Table 1**) were enhanced, reflecting a common strategy applied by phytoplankton in response to higher irradiance (Moisan and Mitchell, 1999; Van Leeuwe et al., 2005; Arrigo et al., 2010; Kroppenske et al., 2010). In line with the latter observation, there was also a light-dependent rise in NPQ, reaching maximum values around 2 in the ML treatment (**Figure 5A**). From ML to HL, a further enhancement of ETR_{max} could be observed in *P. antarctica* (**Table 2**). However, this effect was accompanied by reduced POC production rates (**Figure 2E**) while τ_{Q_a} remained unaltered (**Figure 4A**). Hence, HL resulted in the saturation of the Calvin cycle and therewith the requirement for alternative electron cycling to dissipate the excessive light energy. While cyclic electron transfer is insignificant at low irradiance, it is, however, an important strategy to prevent overexcitation of PSII at high irradiance (Feikema et al., 2006). Higher cyclic electron transport around PSI at HL potentially led to higher production of ATP at the expense of NADPH (Heber et al., 1978; Falk and Palmqvist, 1992) causing thereby the here observed reduction in POC production in *P. antarctica* (**Figure 2E**). Evidence of increased cyclic electron transport was observed particularly in colder habitats (Larkum et al., 2017) and was found to be active under high irradiance in another *P. antarctica* strain (Alderkamp et al., 2012).

The growth and POC production rates of *C. debilis* of the +Fe treatments measured at LL and ML (**Figures 2D,F**) are strongly reduced compared with the previously estimated rates (growth: 0.41 ± 0.06 and 0.87 ± 0.10 d⁻¹ and POC production: 12.3 ± 1.5 and 29.0 ± 3.4 pg C cell⁻¹ d⁻¹ at 20 and 200 $\mu\text{mol photons m}^{-2} \text{ s}^{-1}$, respectively) when this species was grown under the same light levels, but much higher Fe concentrations (12 $\mu\text{mol L}^{-1}$, Trimborn et al., 2017). As the experiments here were conducted with initial Fe concentrations of 2 nmol L⁻¹ in our +Fe treatments, this may indicate that *C. debilis* was already slightly Fe-limited at the end of the experiments in these treatments. This was, however, not the case for *P. antarctica*, which reached similar high growth and POC production rates irrespective of whether it was grown at 2 nmol L⁻¹ (+Fe treatments, **Figures 2C,E**) or 12 $\mu\text{mol L}^{-1}$ dFe (Trimborn et al., 2017). Hence, these results point toward a much higher susceptibility of the diatom to be Fe limited at Fe concentrations, at which the prymnesiophyte remained unaffected. This is in line with previous observations that *P. antarctica* was found to have a higher affinity for Fe binding as well as a lower Fe requirement than SO diatoms (Hassler and Schoemann, 2009; Strzpek et al., 2011).

Considering that *C. debilis* was already slightly limited by Fe in our +Fe treatments, the higher light availability between LL and ML was neither reflected in higher POC production rates (**Figure 2F**) nor in ETR_{max} (**Table 2**), with both parameters remaining unchanged. As the re-oxidation of *Q_a* took longer (**Figure 4B**), slower electron transfer into carbon fixation was indicated. Moreover, *C. debilis* showed signs of light stress at ML, as various photophysiological parameters such as F_v/F_m (**Figure 1B**), the number of functional PSII reaction centers per

cell (RCII, **Table 2**), the functional absorption cross-section of PSII (σ_{PSII}) and the maximum light use efficiency (α , **Table 2**) were all reduced. Hence, *C. debilis* adjusted its physiological state toward a photoprotective state at ML. Accordingly, cell quotas of pigments related to light absorption were strongly lowered between LL and ML (**Table 1**) while those related to photoprotection remained unchanged (**Table 1**), as typically observed for SO diatoms (Van Leeuwe et al., 2005; Arrigo et al., 2010; Kroppenske et al., 2010). Please note that irrespective of the applied light intensity *C. debilis* was characterized by similar high cell quotas of diadinoxanthin (**Table 1**), which compete for photons with the light harvesting pigments, potentially hampering the transfer of the absorbed energy to photochemistry in particular under LL conditions. Between ML and HL, growth remained constant in the +Fe treatments. To diminish light absorption, F_v/F_m and *P* went down toward HL (**Figure 1B** and **Table 2**), reducing therewith the energy transfer between the antennas. The latter seems to be an efficient strategy against high irradiance, as shown by the full recovery of F_v/F_m in the +Fe-HL treatments of *C. debilis* after the FLC curve (**Table 2**). Interestingly, HL led to a stimulation of POC production rates by 42% in *C. debilis* (**Figure 2F**). Next to the faster re-oxidation times of *Q_a* (**Figure 4B**), also ETR_{max} exhibited a strong increase by ~230% between ML and HL (**Table 2**). This indicates strong alternative electron cycling such as Mehler reaction (Mehler, 1957) and cyclic electron flow within PSII (Prasil et al., 1996), which have all been shown to reduce excitation pressure on PSII by providing alternate electron pathways that do not lead to reduction of CO₂, but bearing also the risk of reactive oxygen species formation. In particular active electron transfer cycling around PSII was reported to operate in many diatoms of temperate and polar regions when the plastoquinone pool is reduced as a consequence of exposure to high irradiance (Lavaud et al., 2002; Goldman et al., 2014). Hence, such photoprotection strategies potentially also acted in *C. debilis* efficiently preventing photodamage at high irradiance.

Ample supply of light, Fe or other nutrients was found to promote growth, causing shorter cell cycle duration and therewith less time to take up silicate by diatoms (Martin-Jézéquel et al., 2000). As a consequence less strongly silicified cells are usually observed under such favorable growth conditions (Taylor, 1985; Timmermans et al., 2004; Hoffmann et al., 2007). Under high irradiance, it was previously shown that temperate diatoms such as *Coscinodiscus granii* (Taylor, 1985), *Thalassiosira weissflogii* (Liu et al., 2016) were less silicified. By contrast, cellular BSi concentrations were similar in *Ditylum brightwellii* or enhanced in *Thalassiosira oceanica* under high (75 $\mu\text{mol photons m}^{-2} \text{ s}^{-1}$) compared to low irradiance (7.5 $\mu\text{mol photons m}^{-2} \text{ s}^{-1}$; Bucciarelli et al., 2010), pointing toward interspecific differences in silicification by light. In our study, BSi production rates of the +Fe treatments of *C. debilis* strongly increased with increasing light intensities, reaching highest values at HL (**Figure 2G**). Thicker silica shells could protect this species better against grazing (Hamm et al., 2003; Wilken et al., 2011). Recently, it was also reported that optical properties of the silica valve of pennate temperate diatoms were found to modulate light absorption for efficient photosynthesis (Goessling et al., 2018). For the freshwater diatom *Melosira varians* it was further

proposed that the higher attenuation of the more energetic blue light by the silica valve could protect photosynthesis at high irradiance (Yamanaka et al., 2008). One may speculate whether the here observed increase in frustule thickness of *C. debilis* in response to the increasing irradiance potentially also played a role in photoprotection, a hypothesis that certainly would need further testing. This fits, however, the observation that increased silicification increases sinking to lower mean irradiances with depth (Raven and Waite, 2004).

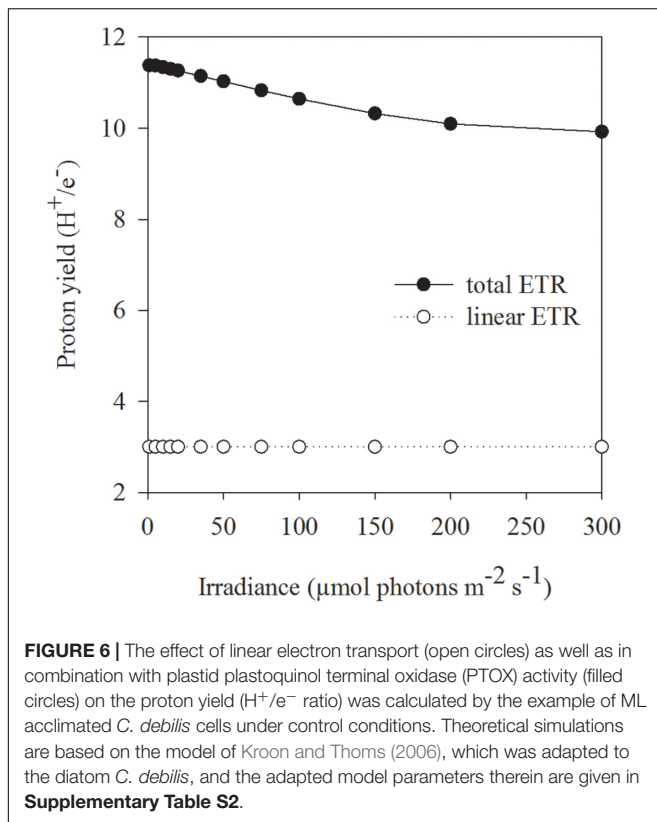
Opposed to the prymnesiophyte, even though Fe was added to the +Fe treatments the diatom *C. debilis* exhibited lowered growth rates as a result from mild Fe limitation. Interestingly, when both species were grown under increasing irradiance, the mildly Fe-limited cells of *C. debilis* were found to have acclimated to the different light conditions in a very efficient way. The diatom successfully prevented photodamage and kept POC production rates constant, pointing toward a high flexibility of this species to cope with HL even when slightly limited by Fe. The prymnesiophyte on the other hand reached maximum growth rates in all light treatments after Fe enrichment and did not show any signs of Fe limitation. When grown at HL, this species also applied efficient photoprotective strategies, but this was at the expense of POC buildup.

***P. antarctica* Is More Tolerant Than *C. debilis* to Fe Limitation and High Light**

Different to previous Fe manipulation experiments with SO phytoplankton species in the laboratory (Timmermans et al., 2001; Hoffmann et al., 2008; Alderkamp et al., 2012; Strzepek et al., 2012; Luxem et al., 2017), we grew our SO phytoplankton isolates in Fe-poor Antarctic seawater (initially total dissolved Fe concentrations of 0.4 nmol L^{-1}) without usage of any chelating agent such as desferrioxamine B (DFB) or ethylenediaminetetraacetic acid (EDTA). For more than a year before the beginning of the experiments, both species were already grown in this seawater, which was enriched with chelexed macronutrients and vitamins and other trace metals (for details see section Materials and Methods). Thus our results represent long term acclimation and no short time responses. Strong Fe limitation of our control treatments for both species was indicated by significant differences in F_v/F_m and σ_{PSII} between control and Fe-enriched treatments (Figure 1). In line with other studies (Greene et al., 1991, 1992; Strzepek et al., 2012), Fe limitation resulted in a significant decline of F_v/F_m while it increased σ_{PSII} in all control treatments of both species. Furthermore, Fe stress was found to decrease the overall photosynthetic capacity (Alderkamp et al., 2012; Behrenfeld and Milligan, 2012; Petrou et al., 2014; Koch et al., 2019), as seen by the significantly reduced POC production rates among all control treatments (Figures 2E,F and Supplementary Table S1), confirming successful achievement of strong Fe limitation in our two species. Similarly, the control treatments of both species displayed both lower biovolume and growth rates than the +Fe treatments (Figures 2A–D). Similar responses to Fe limitation were previously observed for the same (Koch et al., 2019) and other (Alderkamp et al., 2012; Strzepek et al., 2012; Luxem et al., 2017) strains of *P. antarctica* as well as for various

Antarctic diatoms including *Chaetoceros* species (Timmermans et al., 2001; Pankowski and McMinn, 2009; Alderkamp et al., 2012; Strzepek et al., 2012; Petrou et al., 2014).

In line with other studies (Van Leeuwe and Stefels, 1998; Hoffmann et al., 2008; Alderkamp et al., 2012; Luxem et al., 2017), Fe-limited *P. antarctica* cells contained less chlorophyll *a*, decreasing thereby the potential to absorb light (Table 1). On the other hand, the total amount of diadinoxanthin and diatoxanthin relative to chlorophyll (DD + DT):Chl was much higher in control compared to +Fe-treatments (data not shown) suggesting that the Fe-limited *P. antarctica* cells displayed physiological characteristics of high light acclimation, as previously observed for monocultures of *P. antarctica* and diatoms (Van Leeuwe and Stefels, 1998; Alderkamp et al., 2012; Petrou et al., 2014) and natural SO phytoplankton assemblages (Petrou et al., 2011). With increasing light intensity, *P. antarctica* managed to sustain similar high growth rates in control treatments (Figure 2C), indicating that this species was able to cope well with a more Fe economical metabolism also under higher irradiances. As Fe is required in various components of the electron transport chain, low Fe availability can strongly influence photosynthesis. As a consequence from Fe limitation, the combination of large antenna size and temperature-constrained photosynthetic processes ‘downstream’ from light absorption can be disadvantageous in particular in combination with high irradiance (Moore et al., 2007; Hoffmann et al., 2008; Strzepek et al., 2012). Indeed in the control treatment of *P. antarctica* the lowered F_v/F_m (29%, Figure 1A) and [RCII] (44%, Table 2) were counteracted by larger σ_{PSII} (20%, Figure 1C) between LL and ML. As observed before in various SO phytoplankton species (Timmermans et al., 2001; van Oijen et al., 2004; Strzepek et al., 2012; Petrou et al., 2014), the here observed larger antenna complexes in the control treatment of *P. antarctica* potentially compensated for fewer Fe-rich PSII. Opposed to previous assumptions (Moore et al., 2007; Hoffmann et al., 2008; Strzepek et al., 2012), shorter Q_a re-oxidation time (Figure 4A) facilitated faster electron drainage into downstream processes from LL to ML in *P. antarctica*. Fe limited cells of another *P. antarctica* strain (#1871) were also able to efficiently channel electrons from PSII to carbon fixation (Alderkamp et al., 2012). Next to similar high POC production rates (Figure 2E) as well as faster Q_a re-oxidation (Figure 4A), the rise of ETR_{max} by 175% (Table 2) between LL and ML in our control treatment of *P. antarctica* suggests high activities of alternative electron acceptors, which diverted away the excess light energy. The latter findings suggest the operation of pathways such as the Mehler reaction. Moreover, cellular diadinoxanthin concentrations doubled between LL and ML in the control treatments (Table 1), with most of the energy dissipated via NPQ (up to 1, Figure 5B). Similarly, the same and another *P. antarctica* strain relied on high NPQ activity when grown under Fe limitation at $100 \mu\text{mol photons m}^{-2} \text{ s}^{-1}$ (up to 1.5, Koch et al., 2019) and at the average light intensity of the dynamic light cycle of $73 \mu\text{mol photons m}^{-2} \text{ s}^{-1}$ (up to 1, Alderkamp et al., 2012). When the control treatment of *P. antarctica* was grown at HL, however, almost no NPQ could be detected (Figure 5B) while POC production rates (Figure 2E), ETR_{max} (Figure 3B and Table 2) and cellular diadinoxanthin quotas (Table 1) remained the same as when grown at ML.



Therefore, we speculate that other processes than xanthophyll cycling such as cyclic electron transfer around PSI were active at HL to prevent photodamage. Hence, our study clearly shows that Fe-limited *P. antarctica* cells were well protected from photoinhibition against high irradiance levels, providing them an advantage in Fe-poor waters under various light conditions.

In contrast to the tolerant prymnesiophyte, severe Fe limitation strongly amplified the negative effect of increasing light in *C. debilis*, as the cells were unable to grow at HL in the control treatment (Figure 2D). Only under LL and ML, the control treatment of *C. debilis* managed to grow and exhibited similar low growth rates. In line with previous observations (Timmermans et al., 2001; Alderkamp et al., 2012; Strzpek et al., 2012) the strongly lowered F_v/F_m , but increased σ_{PSII} values of the control treatments of *C. debilis* suggest strongly impaired photochemical efficiencies (Figures 1B,D). In fact, carbon fixation was largely hampered in the control treatments at both irradiances, as seen by the low POC production rates for *C. debilis* ($0.6\text{--}0.8 \text{ pg cell}^{-1} \text{ d}^{-1}$, Figure 2F and Supplementary Table S1). Considering that the cell volume of *C. debilis* was three times larger than *P. antarctica* (Figures 2A,B), it is surprising to see that both species displayed similar POC production rates in the control treatments (Figures 2E,F) or that *C. debilis* had even lower rates than *P. antarctica* when normalized per cell volume (Supplementary Table S1). Hence in comparison, control conditions more severely impacted POC build up in *C. debilis* than *P. antarctica*. Similar observations were previously made for the diatom *F. cylindrus* compared to

P. antarctica under Fe-limiting conditions (Alderkamp et al., 2012). Surprisingly, ETR_{max} were similar irrespective of Fe availability (Figures 3C,D). As POC is produced via linear electron transport, the here observed similar high ETR_{max} can be explained by operation of a putative plastid plastoquinol terminal oxidase (PTOX), which creates a proton gradient for ATP synthesis by the release of protons into the thylakoid lumen during water splitting (Mackey et al., 2008). To simulate the high ETRs measured for +Fe and control treatments of *C. debilis* under ML conditions (Figures 3C,D), the model by Kroon and Thoms (2006) was modified for this study to calculate the diatom's ETRs (Supplementary Table S2). As can be seen in Figures 3E,F, the measured ETRs and their light-use characteristics of *C. debilis* under ML conditions (Figures 3C,D and Supplementary Table S3) could be well reproduced for both treatments. Moreover, it becomes evident that only for the control treatments PTOX contributed approximately to 80% relative to the overall ETRs (Figure 3F). In addition to the calculated ETRs for the control treatments of *C. debilis*, we also estimated the contribution of PTOX to the proton yield ($\text{H}^+/\text{linear e}^-$), which is a measure of protons released into the thylakoid lumen per electron transported linearly. Assuming only linear electron transport the proton yield reached ~ 3 whereas PTOX operation increased the yield by a factor of $\sim 3\text{--}4$ times (Figure 6 and Supplementary Figure S1). Hence, as a result from PTOX operation more ATP would be generated per electron transported, as previously suggested by Behrenfeld and Milligan (2012). The model further allowed reassessing the impact of PTOX on Q_a re-oxidation and was found to reproduce well the measured faster re-oxidation times of the control treatment of *C. debilis* (Figure 4B and Supplementary Figure S1). A lower pH in the thylakoid lumen would further facilitate the de-epoxidation of diadinoxanthin into diatoxanthin. High xanthophyll activity by the control treatment of *C. debilis* was given by its high cellular diadinoxanthin content (Table 1) along with very high NPQ activities (Figure 5D). In comparison, the control treatment of *C. debilis* displayed much higher NPQ activities than *P. antarctica*, supporting previous observations that xanthophyll-cycle activity was a very important photoprotection strategy of diatoms (Beer et al., 2011; Alderkamp et al., 2012). Such strategy is especially efficient after short-term exposure to high irradiance, as seen by the high potential of F_v/F_m recovery ($\sim 70\text{--}80\%$, Table 2), pointing toward a high tolerance of *C. debilis* to short-term high light stress.

Based on the study by Boyle (1998), the concept was established that Fe-limited cells have thicker silica shells. For temperate diatoms, however, there was no clear trend with respect to this concept (Marchetti and Harrison, 2007; Bucciarelli et al., 2010). Among the tested Antarctic diatoms, previous findings were confirmed for *Fragilariopsis kerguelensis*, but provided also evidence that independent of Fe limiting conditions the cellular Si content can remain unchanged as in *Corethron pennatum* (Timmermans et al., 2004) or *Chaetoceros dictyota* (Hoffmann et al., 2007). In our study, BSi production rates were similar between control and +Fe treatments when grown at LL, but differed at ML (Figure 2G).

In the latter case, the ML acclimated cells were less silicified in control compared to the +Fe treatment. Among the control treatments of *C. debilis* the degree of silicification was, however, similar irrespective of the growth light intensity, suggesting that this species could be more prone to grazing in Fe-poor waters.

Ecological Implications for the Occurrence of Both Taxa in a Future Southern Ocean

It is currently not well understood how the ongoing climatic changes will affect phytoplankton distribution in the future SO. In this respect, different climatic scenarios are currently envisioned. In the first scenario, as a consequence of rising sea surface temperature the upper water layer could be more stratified hence exposing phytoplankton to a more stable low Fe high light environment (Meijers, 2014; Hauck et al., 2015). Similar to the sea ice diatom *F. cylindrus* (Arrigo et al., 2010; Alderkamp et al., 2012; Goldman et al., 2014), *C. debilis* when grown under control conditions in conjunction with LL and ML exhibited a high photoprotective capacity on short time scales, potentially enabling this species to slowly grow in Fe-deficient waters of low to medium light levels. Considering that *C. debilis* was isolated from the Antarctic polar front where the availability of light and iron can be variable as a result from vertical mixing (Alderkamp et al., 2010), the high photoprotective capacity of this species allowed it to cope well with low Fe concentrations and medium light conditions. *C. debilis* was, however, not well adapted to a future low Fe high light climate scenario as it was unable to grow in the control treatments under HL. Hence, on a long time scale *C. debilis* could not survive in high light Fe-poor waters. In contrast to *C. debilis*, the prymnesiophyte *P. antarctica* was well adapted to thrive in Fe-deficient waters under various light levels, as it was able to maintain constant growth and photosynthesis rates under all light conditions. In line with findings on a different *P. antarctica* strain (Alderkamp et al., 2012), also the here tested strain possessed high photoprotective capabilities, with strong alternative electron cycling activities (electron cycling around PSI, Mehler and/or photorespiration) being more important than xanthophyll cycling. Overall, this study suggests that *P. antarctica* could outcompete *C. debilis* in Fe-deficient waters at all light regimes.

Another climatic scenario predicts an intensification of westerly winds and stronger vertical mixing (Bopp et al., 2001, 2013; Meijers, 2014), therefore SO phytoplankton could encounter less light together with higher Fe supply from deeper layers (Hauck et al., 2015). In such scenario, *P. antarctica* would also outcompete *C. debilis*, as growth rates of the prymnesiophyte were twice as high as the diatom in the +Fe treatments grown at LL. As *C. debilis* was already experiencing mild Fe-limitation in the +Fe treatments, these treatments are rather representative for an occasional sporadic Fe input event. Actually, the here studied *C. debilis* strain was isolated during the EIFEX Fe fertilization study inside an eddy of the Antarctic Polar front with variable environmental conditions (Smetacek et al., 2012).

Indeed, similar growth rates to the ones measured here were previously estimated for *C. debilis* in the field after *in situ* Fe fertilization, during which it became a dominant species (Tsuda et al., 2003; Assmy et al., 2007). Assuming a scenario in which Fe would be constantly supplied, *C. debilis* would reach similar high growth rates as the flagellate under low growth irradiance (Trimborn et al., 2017). Even though the scenario of a higher availability of both light and sporadic Fe input is rather unlikely (Hauck et al., 2015), such combination was, however, found to be beneficial for *C. debilis*, promoting growth, POC and BSi production rates. Similar to Antarctic diatoms such as *Fragilariopsis cylindrus* (Kropuenske et al., 2010; Alderkamp et al., 2012) and *Chaetoceros brevis* (Van de Poll et al., 2011), *C. debilis* showed high photoprotection capacities, pointing toward a high flexibility of this species to cope with HL after Fe enrichment. Under such a scenario, *C. debilis* would reach similar high growth rates as *P. antarctica*, but in comparison the diatom would produce relatively more carbon than the flagellate. Due to its much thicker silica shell under these conditions, it would be well protected against grazers, so that chances of efficient carbon export would be much higher for the diatom whereas flagellates are more likely to be grazed, contributing therewith rather to carbon remineralization. Considering, however, that it is more realistic to assume a low Fe high light climate scenario, this suggests rather a decline in diatom abundance with a shift toward flagellates in the future, with significant consequences for biogeochemical cycling, including Fe remineralization and carbon and silicate drawdown.

AUTHOR CONTRIBUTIONS

SB acquired the presented data. SB and ScT designed the study. SiT, SB, and ScT analyzed and interpreted the data. ScT wrote the manuscript with critical feedback from all co-authors.

FUNDING

ScT was funded by the Helmholtz Impulse Fond (HGF Young Investigators Group *EcoTrace*, VH-NG-901). SB was funded by the Deutsche Forschungsgemeinschaft (DFG) in the framework of the priority programme ‘*Antarctic Research with comparative investigations in Arctic ice areas*’, grant no. BE5105/1-1.

ACKNOWLEDGMENTS

M. Rizkallah, T. Brenneis, Britta Meyer-Schlosser, and J. P. Heiden are thanked for the support in the laboratory.

SUPPLEMENTARY MATERIAL

The Supplementary Material for this article can be found online at: <https://www.frontiersin.org/articles/10.3389/fmars.2019.00167/full#supplementary-material>

REFERENCES

- Alderkamp, A.-C., de Baar, H. J. W., Visser, R. J. W., and Arrigo, K. R. (2010). Can photoinhibition control phytoplankton abundance in deeply mixed water columns of the Southern Ocean? *Limnol. Oceanogr.* 55, 1248–1264. doi: 10.4319/lo.2010.55.3.1248
- Alderkamp, A.-C., Kulk, G., Buma, A. G. J., Visser, R. J. W., Van Dijken, G. L., Mills, M., et al. (2012). The effect of iron limitation on the photophysiology of *Phaeocystis antarctica* (Prymnesiophyceae) and *Fragilariopsis cylindrus* (Bacillariophyceae) under dynamic irradiance. *J. Phycol.* 48, 45–59. doi: 10.1111/j.1529-8817.2011.01098.x
- Arrigo, K. R., Mills, M. M., Kropuenske, L. R., Van Dijken, G. L., Alderkamp, A. C., and Robinson, D. H. (2010). Photophysiology in two major southern ocean phytoplankton taxa: photosynthesis and growth of *Phaeocystis antarctica* and *Fragilariopsis cylindrus* under different irradiance levels. *Integr. Comp. Biol.* 50, 950–966. doi: 10.1093/icb/icc021
- Assmy, P., Henjes, J., Klaas, C., and Smetacek, V. (2007). Mechanisms determining species dominance in a phytoplankton bloom induced by the iron fertilization experiment EisenEx in the Southern Ocean. *Deep Sea Res. Part I Oceanogr. Res. Pap.* 54, 340–362. doi: 10.1016/j.dsr.2006.12.005
- Beer, A., Juhas, M., and Büchel, C. (2011). Influence of different light intensities and iron nutrition on the photosynthetic apparatus in the diatom *Cyclotella menghiana* (Bacillariophyceae). *J. Phycol.* 47, 1266–1273. doi: 10.1111/j.1529-8817.2011.01060.x
- Behrenfeld, M. J., and Milligan, A. J. (2012). Photophysiological expressions of iron stress in phytoplankton. *Ann. Rev. Mar. Sci.* 5, 217–246. doi: 10.1146/annurev-marine-121211-172356
- Bopp, L., Monfray, P., Aumont, O., Dufresne, J.-L., LeTreut, H., Madec, G., et al. (2001). Potential impact of climate change on marine export production. *Glob. Biogeochem. Cyc.* 15, 81–99. doi: 10.1029/1999GB001256
- Bopp, L., Resplandy, L., Orr, J. C., Doney, S. C., Dunne, J. P., Gehlen, M., et al. (2013). Multiple stressors of ocean ecosystems in the 21st century: projections with CMIP5 models. *Biogeosciences* 10, 6225–6245. doi: 10.5194/bg-10-6225-2013
- Boyle, E. (1998). Pumping iron makes thinner diatoms. *Nature* 393, 733–734. doi: 10.1038/31585
- Brzezinski, M. A., and Nelson, D. M. (1995). The annual silica cycle in the Sargasso Sea near Bermuda. *Deep Sea Res. Part I Oceanogr. Res. Pap.* 42, 1215–1237. doi: 10.1016/0967-0637(95)93592-3
- Bucciarelli, E., Pondaven, P., and Sarthou, G. (2010). Effects of an iron-light co-limitation on the elemental composition (Si, C, N) of the marine diatoms *Thalassiosira oceanica* and *Ditylum brightwellii*. *Biogeosciences* 7, 657–669. doi: 10.5194/bg-7-657-2010
- Dunne, J. P., Sarmiento, J. L., and Gnanadesikan, A. (2007). A synthesis of global particle export from the surface ocean and cycling through the ocean interior and on the seafloor. *Glob. Biogeochem. Cycles* 21:GB4006. doi: 10.1029/2006GB002907
- Falk, S., and Palmqvist, K. (1992). Photosynthetic light utilization efficiency, photosystem II heterogeneity, and fluorescence quenching in *Chlamydomonas reinhardtii* during the induction of the CO₂-concentrating mechanism. *Plant Physiol.* 100, 685–691. doi: 10.1104/pp.100.2.685
- Falkowski, P. G., and Raven, J. A. (2007). *Aquatic Photosynthesis*. Princeton, NJ: Princeton University Press.
- Feikema, W. O., Marosvolgyi, M. A., Lavaud, J., and Van Gorkom, H. J. (2006). Cyclic electron transfer in photosystem II in the marine diatom *Phaeodactylum tricornerutum*. *Biochim. Biophys. Acta* 1757, 829–834. doi: 10.1016/j.bbabo.2006.06.003
- Genty, B., Briantais, J.-M., and Baker, N. R. (1989). The relationship between the quantum yield of photosynthetic electron transport and quenching of chlorophyll fluorescence. *Biochim. Biophys. Acta* 990, 87–92. doi: 10.1016/S0304-4165(89)80016-9
- Gerringa, L. J. A., de Baar, H. J. W., and Timmermans, K. R. (2000). A comparison of iron limitation of phytoplankton in natural oceanic waters and laboratory media conditioned with EDTA. *Mar. Chem.* 68, 335–346. doi: 10.1016/S0304-4203(99)00092-4
- Goessling, J. W., Frankenbach, S., Ribeiro, L., Seródio, J., and Kühl, M. (2018). Modulation of the light field related to valve optical properties of raphid diatoms: implications for niche differentiation in the microphytobenthos. *Mar. Ecol. Prog. Ser.* 588, 29–42. doi: 10.3354/meps12456
- Goldman, J. A. L., Kranz, S. A., Young, Y. N., Tortell, P. D., Stanley, R. H. R., Bender, M. L., et al. (2014). Gross and net production during the spring bloom along the Western Antarctic Peninsula. *New Phytol.* 205, 182–191. doi: 10.1111/nph.13125
- Greene, R. M., Geider, R. J., and Falkowski, P. G. (1991). Effect of iron limitation on photosynthesis in a marine diatom. *Limnol. Oceanogr.* 36, 1772–1782. doi: 10.4319/lo.1991.36.8.1772
- Greene, R. M., Geider, R. J., Kolber, Z., and Falkowski, P. G. (1992). Iron-induced changes in light harvesting and photochemical energy conversion processes in eukaryotic marine algae. *Plant Physiol.* 100, 565–575. doi: 10.1104/pp.100.2.565
- Guillard, R. R. L., and Ryther, J. H. (1962). Studies of marine planktonic diatoms: I. *Cyclotella nana* Hustedt, and *Detonula confervacea* (Cleve) Grun. *Can. J. Microbiol.* 8, 229–239. doi: 10.1139/m62-029
- Hamm, C. E., Merkel, R., Springer, O., Jurkoic, P., Maier, C. R., Prechtel, K., et al. (2003). Architecture and material properties of diatom shells provide effective mechanical protection. *Nature* 421, 841–843. doi: 10.1038/nature01416
- Hassler, C. S., and Schoemann, V. (2009). Bioavailability of organically bound Fe to model phytoplankton of the Southern Ocean. *Biogeosciences* 6, 2281–2296. doi: 10.5194/bg-6-2281-2009
- Hauk, J., Völker, C., Wolf-Gladrow, D. A., Laufkötter, C., Vogt, M., Aumont, O., et al. (2015). On the Southern Ocean CO₂ uptake and the role of the biological carbon pump in the 21st century. *Glob. Biogeochem. Cycles* 29, 1451–1470. doi: 10.1002/2015GB005140
- Heber, U., Egneus, H., Hanck, U., Jensen, M., and Koster, S. (1978). Regulation of photosynthetic electron-transport and photophosphorylation in intact chloroplasts and leaves of *Spinacia oleracea* L. *Planta* 143, 41–49. doi: 10.1007/BF00389050
- Heiden, J. P., Bischof, K., and Trimborn, S. (2016). Light intensity modulates the response of two Antarctic diatom species to ocean acidification. *Front. Mar. Sci.* 3:260. doi: 10.3389/fmars.2016.00260
- Heiden, J. P., Thoms, S., Bischof, K., and Trimborn, S. (2018). Ocean acidification stimulates particulate organic carbon accumulation in two Antarctic diatom species under moderate and high solar radiation. *J. Phycol.* 54, 505–517. doi: 10.1111/jpy.12753
- Hillebrand, H., Dürselen, C.-D., Kirschtel, D., Pollinger, U., and Zohary, T. (1999). Biovolume calculation for pelagic and benthic microalgae. *J. Phycol.* 35, 403–424. doi: 10.1046/j.1529-8817.1999.3520403.x
- Hoffmann, L. J., Peeken, I., and Lochte, K. (2007). Effects of iron on the elemental stoichiometry during EIFEX and in the diatoms *Fragilariopsis kerguelensis* and *Chaetoceros dichaeta*. *Biogeosciences* 4, 569–579. doi: 10.5194/bg-4-569-2007
- Hoffmann, L. J., Peeken, I., and Lochte, K. (2008). Iron, silicate, and light co-limitation of three Southern Ocean diatom species. *Polar Biol.* 31, 1067–1080. doi: 10.1007/s00300-008-0448-6
- Koch, F., Beszteri, S., Harms, L., and Trimborn, S. (2019). The impacts of iron limitation and ocean acidification on the cellular stoichiometry, photophysiology and transcriptome of *Phaeocystis antarctica*. *Limnol. Oceanogr.* 64, 357–375. doi: 10.1002/lno.11045
- Kolber, Z. S., Prášil, O., and Falkowski, P. G. (1998). Measurements of variable chlorophyll fluorescence using fast repetition rate techniques: defining methodology and experimental protocols. *Biochim. Biophys. Acta* 1367, 88–106. doi: 10.1016/S0005-2728(98)00135-2
- Koroleff, F. (1983). “Determination of silicon,” in *Methods of Seawater Analysis*, eds K. Grasshoff and M. Kremling (Weinheim: Wiley-VCH), 174–183.
- Kroon, B. M. A., and Thoms, S. (2006). From electron to biomass: a mechanistic model to describe phytoplankton photosynthesis and steady-state growth rates. *J. Phycol.* 42, 593–609. doi: 10.1111/j.1529-8817.2006.00221.x
- Kropuenske, L. R., Mills, M. M., van Dijken, G. L., Alderkamp, A.-C., Mine Berg, G., Robinson, D. H., et al. (2010). Strategies and rates of photoacclimation in two major Southern Ocean phytoplankton taxa: *Phaeocystis antarctica* (Haptophyta) and *Fragilariopsis cylindrus* (Bacillariophyceae). *J. Phycol.* 46, 1138–1151. doi: 10.1111/j.1529-8817.2010.00922.x
- Landschützer, P., Gruber, N., Haumann, F. A., Rödenbeck, C., Bakker, D. C. E., Van Heuven, S., et al. (2015). The reinvigoration of the Southern Ocean carbon sink. *Science* 349, 1221–1224. doi: 10.1126/science.aab2620

- Larkum, A. W. D., Szabo, M., Fitzpatrick, D., and Raven, J. A. (2017). "Cyclic electron flow in cyanobacteria and eukaryotic algae," in *Photosynthesis and Bioenergetics*, eds J. Barber and A. V. Ruban (Singapore: World Scientific Publishing Company Pte Limited), 305–343. doi: 10.1142/9789813230309-0014
- Lavaud, J., Van Gorkom, H. J., and Etienne, A. L. (2002). Photosystem II electron transfer cycle and chlororespiration in planktonic diatoms. *Photosynth. Res.* 74, 51–59. doi: 10.1023/A:1020890625141
- Liu, H., Chen, M., Zhu, F., and Harrison, P. J. (2016). Effect of diatom silica content on copepod grazing, growth and reproduction. *Front. Mar. Sci.* 3:89. doi: 10.3389/fmars.2016.00089
- Luxem, K. E., Ellwood, M. J., and Strzepek, R. F. (2017). Intraspecific variability in *Phaeocystis antarctica*'s response to iron and light stress. *PLoS One* 12:e0179751. doi: 10.1371/journal.pone.0179751
- Mackey, K. R. M., Paytan, A., Grossman, A. R., and Bailey, S. (2008). A photosynthetic strategy for coping in a high-light, low-nutrient environment. *Limnol. Oceanogr.* 53, 900–913. doi: 10.4319/lo.2008.53.3.0900
- Marchetti, A., and Harrison, P. J. (2007). Coupled changes in the cell morphology and the elemental (C, N, and Si) composition of the pennate diatom *Pseudonitzschia* due to iron deficiency. *Limnol. Oceanogr.* 52, 2270–2284. doi: 10.4319/lo.2007.52.5.2270
- Martin, J. H., Gordon, R. M., and Fitzwater, S. E. (1990). Iron in Antarctic waters. *Nature* 345, 156–158. doi: 10.1038/345156a0
- Martin-Jézéquel, V., Hildebrand, M., and Brzezinski, M. A. (2000). Silicon metabolism in diatoms: implications for growth. *J. Phycol.* 36, 821–840. doi: 10.1046/j.1529-8817.2000.00019.x
- Mehler, A. H. (1957). Studies on reactions of illuminated chloroplasts. I. Mechanism of the reduction of oxygen and other Hill reagents. *Arch. Biochem. Biophys.* 33, 65–77. doi: 10.1016/0003-9861(51)90082-3
- Meijers, A. J. S. (2014). The Southern Ocean in the coupled model intercomparison project phase 5. *Phil. Trans. R. Soc. A* 372:20130296. doi: 10.1098/rsta.2013.0296
- Mills, M. M., Kropuenske, L. R., van Dijken, G. L., Alderkamp, A.-C., Berg, G. M., Robinson, D. H., et al. (2010). Photophysiology in two Southern Ocean phytoplankton taxa: photosynthesis of *Phaeocystis antarctica* (Prymnesiophyceae) and *Fragilariopsis cylindrus* (Bacillariophyceae) under simulated mixed-layer irradiance. *J. Phycol.* 46, 1114–1127. doi: 10.1111/j.1529-8817.2010.00923.x
- Moisan, T. A., and Mitchell, B. G. (1999). Photophysiological acclimation of *Phaeocystis antarctica* karsten under light limitation. *Limnol. Oceanogr.* 44, 247–258. doi: 10.4319/lo.1999.44.2.0247
- Moore, C. M., Seeyave, S., Hickman, A. E., Allen, J. T., Lucas, M. I., Planquette, H., et al. (2007). Iron-light interactions during the CROZet natural iron bloom and EXport experiment (CROZEX) I: phytoplankton growth and photophysiology. *Deep Sea Res. Part II Top. Stud. Oceanogr.* 54, 2045–2065. doi: 10.1016/j.dsr2.2007.06.015
- Oxborough, K., Moore, C. M., Suggett, D. J., Lawson, T., Chan, H. G., and Geider, R. J. (2012). Direct estimation of functional PSII reaction center concentration and PSII electron flux on a volume basis: a new approach to the analysis of fast repetition rate fluorometry (FRRF) data. *Limnol. Oceanogr. Methods* 10, 142–154. doi: 10.4319/lo.2012.10.142
- Pankowski, A., and McMin, A. (2009). Iron availability regulates growth, photosynthesis, and production of ferredoxin and flavodoxin in Antarctic sea ice diatoms. *Aquat. Biol.* 4, 273–288. doi: 10.3354/ab00116
- Petrou, K., Hassler, C. S., Doblin, M. A., Shelly, K., Schoemann, V., van den Enden, R., et al. (2011). Iron-limitation and high light stress on phytoplankton populations from the Australian Sub-Antarctic Zone (SAZ). *Deep-Sea Res. Part II Top. Stud. Oceanogr.* 58, 2200–2211. doi: 10.1016/j.dsr2.2011.05.020
- Petrou, K., Trimborn, S., Rost, B., Ralph, P. J., and Hassler, C. S. (2014). The impact of iron limitation on the physiology of the antarctic diatom *Chaetoceros simplex*. *Mar. Biol.* 4, 925–937. doi: 10.1007/s00227-014-2392-z
- Prasil, O., Kolber, Z., Berry, J. A., and Falkowski, P. G. (1996). Cyclic electron flow around photosystem II in vivo. *Photosynth. Res.* 48, 395–410. doi: 10.1007/BF00029472
- Ralph, P. J., and Gademann, R. (2005). Rapid light curves: a powerful tool to assess photosynthetic activity. *Aquat. Bot.* 82, 222–237. doi: 10.1016/j.aquabot.2005.02.006
- Raven, J. A. (1990). Predictions of Mn and Fe use efficiencies of phototrophic growth as a function of light availability for growth and of C assimilation pathway. *New Phytol.* 116, 1–18. doi: 10.1111/j.1469-8137.1990.tb00505.x
- Raven, J. A., and Waite, A. M. (2004). The evolution of silicification in diatoms: inescapable sinking or sinking to escape? *New Phytol.* 162, 45–61. doi: 10.1111/j.1469-8137.2004.01022.x
- Robinson, D. H., Kolber, Z., and Sullivan, C. W. (1997). Photophysiology and photoacclimation in surface sea ice algae from McMurdo Sound, Antarctica. *Mar. Ecol. Prog. Ser.* 147, 243–256. doi: 10.3354/meps147243
- Sabine, C. L., Feely, R. A., Gruber, N., Key, R. M., Lee, K., Bullister, J. L., et al. (2004). The oceanic sink for anthropogenic CO₂. *Science* 305, 367–371. doi: 10.1126/science.1097403
- Schuback, N., Schallenberg, C., Duckham, C., Maldonado, M. T., and Tortell, P. D. (2015). Interacting effects of light and iron availability on the coupling of photosynthetic electron transport and CO₂-assimilation in marine phytoplankton. *PLoS One* 10:e0133235. doi: 10.1371/journal.pone.0133235
- Smetacek, V., Klaas, C., Strass, V. H., Assmy, P., Montresor, M., Cisewski, B., et al. (2012). Deep carbon export from a Southern Ocean iron-fertilized diatom bloom. *Nature* 487, 313–319. doi: 10.1038/nature11229
- Strzepek, R. F., Hunter, K. A., Frew, R. D., Harrison, P. J., and Boyd, P. W. (2012). Iron-light interactions differ in Southern Ocean phytoplankton. *Limnol. Oceanogr.* 57, 1182–1200. doi: 10.4319/lo.2012.57.4.1182
- Strzepek, R. F., Maldonado, M. T., Hunter, K. A., Frew, R. D., and Boyd, P. W. (2011). Adaptive strategies by Southern Ocean phytoplankton to lessen iron limitation: uptake of organically complexed iron and reduced cellular iron requirements. *Limnol. Oceanogr.* 56, 1983–2002. doi: 10.4319/lo.2011.56.6.1983
- Suggett, D. J., MacIntyre, H. L., and Geider, R. J. (2004). Evaluation of biophysical and optical determinations of light absorption by photosystem II in phytoplankton. *Limnol. Oceanogr. Methods* 2, 316–332. doi: 10.4319/lo.2004.2.316
- Suggett, D. J., Moore, C. M., Hickman, A. E., and Geider, R. J. (2009). Interpretation of fast repetition rate (FRR) fluorescence: signatures of phytoplankton community structure versus physiological state. *Mar. Ecol. Prog. Ser.* 376, 1–19. doi: 10.3354/meps07830
- Sunda, W. G., and Huntsman, S. A. (1997). Interrelated influence of iron, light and cell size on marine phytoplankton growth. *Nature* 390, 389–392. doi: 10.1038/37093
- Sunda, W. G., and Huntsman, S. A. (2011). Interactive effects of light and temperature on iron limitation in a marine diatom: implications for marine productivity and carbon cycling. *Limnol. Oceanogr.* 56, 1475–1488. doi: 10.4319/lo.2011.56.4.1475
- Taylor, N. J. (1985). Silica incorporation in the diatom *Coscinodiscus granii* is affected by light intensity. *Brit. Phycol. J.* 20, 365–374. doi: 10.1080/00071618500650371
- Timmermans, K. R., Davey, M. S., Van der Wagt, B., Snoek, J., Geider, R. J., Veldhuis, M. J. W., et al. (2001). Co-limitation by iron and light of *Chaetoceros brevis*, *C. dichæta* and *C. calcitrans* (Bacillariophyceae). *Mar. Ecol. Prog. Ser.* 217, 287–297. doi: 10.3354/meps217287
- Timmermans, K. R., van der Wagt, B., and de Baar, H. J. W. (2004). Growth rates, half-saturation constants, and silicate, nitrate, and phosphate depletion in relation to iron availability of four large, open-ocean diatoms from the Southern Ocean. *Limnol. Oceanogr.* 49, 2141–2151. doi: 10.4319/lo.2004.49.6.2141
- Trimborn, S., Thoms, S., Brenneis, T., Heiden, J. P., Beszteri, S., and Bischof, K. (2017). Two Southern Ocean diatoms are more sensitive to ocean acidification and changes in irradiance than the prymnesiophyte *Phaeocystis antarctica*. *Physiol. Plant.* 160, 155–170. doi: 10.1111/pp.12539
- Tsuda, A., Takeda, S., Saito, H., Nishioka, J., Nojiri, Y., Kudo, I., et al. (2003). A mesoscale iron enrichment in the western subarctic Pacific induces a large centric diatom bloom. *Science* 300, 958–961. doi: 10.1126/science.1082000
- Utermöhl, H. (1958). Zur Vervollkommnung der quantitativen Phytoplankton-Methodik. *Mitt. Int. Verein. Theor. Angew. Limnol.* 9, 1–38. doi: 10.1080/05384680.1958.11904091
- Van de Poll, W., Lagunas, M., de Vries, T., Visser, R. J. W., and Buma, A. G. J. (2011). Non-photochemical quenching of chlorophyll fluorescence and xanthophyll cycle responses after excess PAR and UVR in *Chaetoceros brevis*,

- Phaeocystis antarctica and coastal Antarctic phytoplankton. *Mar. Ecol. Prog. Ser.* 426, 119–131. doi: 10.3354/meps09000
- Van Leeuwe, M. A., and Stefels, J. (1998). Effects of iron and light stress on the biochemical composition of Antarctic Phaeocystis sp. (Prymnesiophyceae). II. Pigment composition. *J. Phycol.* 34, 496–503. doi: 10.1046/j.1529-8817.1998.340496.x
- Van Leeuwe, M. A., van Sikkelerus, B., Gieskes, W. W. C., and Stefels, J. (2005). Taxon-specific differences in photoacclimation to fluctuating irradiance in an Antarctic diatom and a green flagellate. *Mar. Ecol. Prog. Ser.* 288, 9–19. doi: 10.3354/meps288009
- van Oijen, T., van Leeuwe, M. A., Gieskes, W. W. C., and de Baar, H. J. W. (2004). Effects of iron limitation on photosynthesis and carbohydrate metabolism in the Antarctic diatom *Chaetoceros brevis* (Bacillariophyceae). *Eur. J. Phycol.* 39, 161–171. doi: 10.1080/0967026042000202127
- Wilken, S., Hoffmann, B., Hersch, N., Kirchgessner, N., Dieluweit, S., Rubner, W., et al. (2011). Diatom frustules show increased mechanical strength and altered valve morphology under iron limitation. *Limnol. Oceanogr.* 56, 1399–1410. doi: 10.4319/lo.2011.56.4.1399
- Wright, S. W., Jeffrey, S. W., Mantoura, R. F. C., Llewellyn, C. A., Bjornland, T., Repeta, D., et al. (1991). Improved HPLC method for the analysis of chlorophylls and carotenoids from marine phytoplankton. *Mar. Ecol. Prog. Ser.* 77, 183–196. doi: 10.3354/meps077183
- Yamanaka, S., Yano, R., Usami, H., Hayashida, N., Ohguchi, M., Takeda, H., et al. (2008). Optical properties of diatom silica frustule with special reference to blue light. *J. Appl. Phys.* 103, 1–6. doi: 10.1063/1.2903342

Conflict of Interest Statement: The authors declare that the research was conducted in the absence of any commercial or financial relationships that could be construed as a potential conflict of interest.

Copyright © 2019 Trimborn, Thoms, Bischof and Beszteri. This is an open-access article distributed under the terms of the Creative Commons Attribution License (CC BY). The use, distribution or reproduction in other forums is permitted, provided the original author(s) and the copyright owner(s) are credited and that the original publication in this journal is cited, in accordance with accepted academic practice. No use, distribution or reproduction is permitted which does not comply with these terms.